Earth Return Aerocapture for the TransHab/Ellipsled Vehicle
Final Study Report for NASA Grant NAG1-2163

Prepared By:

W.D. Muth
C. Hoffmann
&
J.E. Lyne

The University of Tennessee at Knoxville
Aerospace Engineering

October 2000

Abstract

The current architecture being considered by NASA for a human Mars mission involves the use of an aerocapture procedure at Mars arrival and possibly upon Earth return. This technique would be used to decelerate the vehicles and insert them into their desired target orbits, thereby eliminating the need for propulsive orbital insertions. The crew may make the interplanetary journey in a large, inflatable habitat known as the TransHab. It has been proposed that upon Earth return, this habitat be captured into orbit for use on subsequent missions. In this case, the TransHab would be complimented with an aeroshell, which would protect it from heating during the atmospheric entry and provide the vehicle with aerodynamic lift. The aeroshell has been dubbed the "Ellipsled" because of its characteristic shape. This paper reports the results of a preliminary study of the aerocapture of the TransHab/Ellipsled vehicle upon Earth return. Undershoot and overshoot boundaries have been determined for a range of entry velocities, and the effects of variations in the atmospheric density profile, the vehicle deceleration limit, the maximum vehicle roll rate, the target orbit, and the vehicle ballistic coefficient have been examined. A simple, 180 degree roll maneuver was implemented in the undershoot trajectories to target the desired 407 km circular Earth orbit. A three-roll sequence was developed to target not only a specific orbital energy, but also a particular inclination, thereby decreasing propulsive inclination changes and post-aerocapture delta-V requirements. Results show that the TransHab/Ellipsled vehicle has a nominal corridor width of at least 0.7 degrees for entry speeds up to 14.0 km/s. Most trajectories were simulated using continuum flow aerodynamics, but the impact of high-altitude viscous effects was evaluated and found to be minimal. In addition, entry corridor comparisons

have been made between the TransHab/Ellipsled and a modified Apollo capsule which is also being considered as the crew return vehicle; because of its slightly higher lift-to-drag ratio, the TransHab has a modest advantage with regard to corridor width. Stagnation-point heating rates and integrated heat loads were determined for a range of vehicle ballistic coefficients and entry velocities.

Using the arrival vector for a 2020 fast-transit return, trajectories were run beginning at the edge of Earth's sphere of influence. This assured that these simulations used realistic entry latitude/azimuth combinations, while targeting orbits of specific inclinations. For this particular case (in which the arrival declination was –0.7 degrees and the atmospheric entry speed was 11.91 km/s), using the three-roll sequence and an appropriate choice of the azimuth at the edge of the SOI, the vehicle was able to reach circular parking orbits with inclinations ranging from 5.3 to 51.6 degrees. In addition, it was shown that capture into a highly elliptical parking orbit may be feasible. Such a strategy would reduce the integrated heat load during aerocapture and result in a lower ΔV for the trans-Mars injection at the next mission opportunity, but would require precise alignment of the capture orbit with respect to the departure hyperbola for the subsequent mission.

Preliminary work has been done to evaluate the ability of an aerocapture maneuver to target not only a specific orbital energy and inclination, but also a particular longitude of the ascending node; it was found that the current roll control strategy is able to influence the LAN only slightly. The implementation of a blended roll/pitch control algorithm similar to that developed by Jits and Walberg for Mars aerocapture might improve targeting ability and give more control over longitude of the ascending node.

Study Objectives

This document presents results of a preliminary study of the aerocapture of the TransHab/Ellipsled vehicle upon Earth return from a Mars mission. The primary objectives of this study were:

1. to determine the undershoot and overshoot boundaries and the corresponding corridor width as a function of entry velocity;

2. to perform initial studies of stagnation-point heating rates and integrated heat load for the TransHab aerocapture;

3. to determine the influence of variations in the atmospheric density profile, the vehicle deceleration limit, the maximum vehicle roll rate, the target orbit, and the ballistic coefficient on the entry corridor and stagnation-point heating;

4. to compare the nominal entry corridor of the TransHab/Ellipsled vehicle to that of an Apollo-derived capsule which is also being considered for crew return;

5. to evaluate the effect of high-altitude viscous effects (transitional and free-molecular flow) on the TransHab/Ellipsled aerocapture trajectories, and

6. to evaluate the post-aerocapture delta-V requirements and to develop a roll control strategy to target the vehicle into an orbit with a specific inclination and energy, while minimizing the delta-V required for final orbital adjustments. This phase was extended to include an evaluation of the feasibility of targeting longitude of the ascending node as well as inclination and energy.

Vehicle Specifications

TransHab/Ellipsled Vehicle

The TransHab/Ellipsled vehicle is shown in Figure 1. It has a nominal mass of 25,500 kg; the aerodynamic reference area of the vehicle is 84.34 square meters, and the nose radius is 6.7 meters. The TransHab portion of the vehicle has a mass of 14,522 kg. The Ellipsled aeroshell has a mass of 3929 kg, which translates into a mass fraction of 15.4%. The remaining 7053 kg is comprised of various data and communication equipment, batteries and solar arrays, radiator and thermal control systems, and propulsion components. (Vehicle mass data was provided by NASA LARC.)

Table 1 shows the aerodynamic characteristics of the TransHab/Ellipsled vehicle as determined by Gerald LeBeau of NASA Johnson Space Center. The aerodynamic characteristics were calculated using Modified Newtonian theory in which all values are assumed constant at Mach numbers above 24. The table shows that the trim angle of attack is approximately 45 degrees, and the lift-to-drag ratio for Mach 24 and above is 0.39. For comparison purposes, the Apollo capsule derivative, which has also been considered for the crew return vehicle, has a lift-to-drag ratio of approximately 0.3. Therefore, it appears that the TransHab/Ellipsled vehicle should have at least slightly better maneuverability than the Apollo-style capsule.

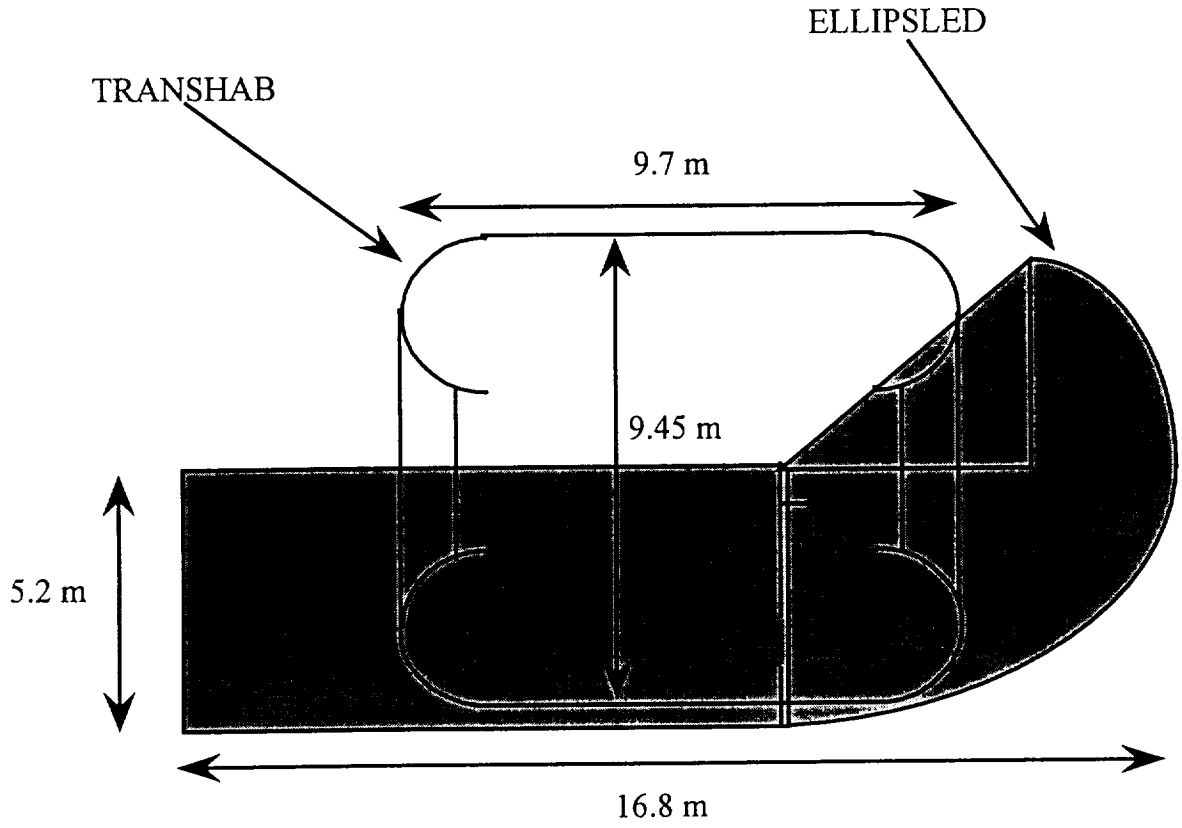

Figure 1. Schematic of the TransHab/Ellipsled vehicle

Table 1. Aerodynamic Characteristics of TransHab/Ellipsled Vehicle

Mach Number	Trim Angle-of-Attack	Lift Coefficient	Drag Coefficient	L/D
2.0	37.12	0.6899	1.5760	0.438
3.0	40.68	0.6317	1.5576	0.406
5.0	43.53	0.5658	1.5128	0.374
10.0	44.6	0.5476	1.4676	0.373
15.0	45	0.5493	1.4623	0.376
24 & above	45	0.5636	1.4445	0.39

Apollo-Derived Vehicle

In addition to the analysis for the TransHab/Ellipsled vehicle, a short study on an Apollo-derived capsule was also performed for comparison purposes. This vehicle is essentially a scaled-up version of the capsules used during the lunar missions. The vehicle has a mass of 6500 kg, a reference length of 4.42 meters, and a surface area of 15.34 square meters. (Again, vehicle data was supplied by LARC.) The coordinate system was altered from that of the original vehicle as well; this resulted in the vehicle having a hypersonic trim angle of approximately 23 degrees. The aerodynamic coefficients were assumed to be constant, and the values of the lift and drag coefficients were determined from a curve fit of the Modified Newtonian data shown in Table 2. The lift coefficient was found to be 0.466 while the drag coefficient was 1.269.

Table 2. Aerodynamic Characteristics of Apollo-Derived Vehicle

Angle-of-Attack	Lift Coefficient	Drag Coefficient	L/D
0	0	1.6	0
5	0.12	1.59	0.075
10	0.23	1.54	0.149
15	0.33	1.46	0.226
20	0.41	1.36	0.301
25	0.49	1.25	0.392
30	0.53	1.10	0.482
35	0.55	0.96	0.572
40	0.54	0.83	0.651

Methodology

The results contained in this paper were obtained using a FORTRAN computer code called the Program to Optimize Simulated Trajectories (POST, Reference 1). The program runs in a UNIX-based environment and consists of an input deck, program files, and various output files. The input deck contains all of the user-defined variables for the trajectory simulations. The user may alter the vehicle configuration, entry condition, integration scheme, and various other simulation properties by making the appropriate changes to the POST input deck. The three degree-of-freedom version of POST was used. For the simulations performed in this study, a fourth order Runga-Kutta integration technique was chosen for the atmospheric portion of the trajectories. The integration time step was set at one second to achieve satisfactory accuracy during the atmospheric portion of the trajectory. In later simulations in which orbital maneuvers were being performed, the integration scheme was changed to an Encke method once the vehicle exited the atmosphere. The time step was also increased to reduce CPU time. The aerodynamic coefficients were input as tables in which the independent variable was Mach number and the dependent variables were the coefficients of lift and drag. For nominal conditions, Earth's atmosphere was modeled using the 1976 U.S. Standard Atmosphere. Atmospheric dispersions were modeled with simple density multipliers, scaling the density at a given altitude to either 70% or 130% of its nominal value. The effects of winds and horizontal density waves were not considered. The Earth was modeled as an oblate planet with the proper harmonic values in the gravity potential function. For most cases, atmospheric entry was considered to occur at an altitude of

121,900 meters, and this is the altitude at which the entry angles and velocities are specified. The maximum deceleration was not allowed to exceed 5 G during a trajectory. The nominal target orbit was circular with an altitude of 407 km. Because of the large size of the vehicle, the roll rates were limited to either 5 or 10 degrees per second. (Unless otherwise stated, the 10-degree per second maximum was used.)

Convective heating rates were calculated with the Chapman relationship supplied in 3D POST. The radiative heating was calculated using a bi-variant table lookup procedure in POST. The data used to create this table was taken from Sutton *et al.* (Ref. 2). Heating rates were interpolated from the Sutton data for a nose radius of 6.7 meters, and these were input to POST as a function of both density and atmospheric relative velocity. A zero radiative heating rate was specified at extremely low densities (altitudes above 84 km) and speeds below 9 km/s to insure that POST did not extrapolate incorrectly. The implementation of these modifications had no significant effect on the maximum stagnation point heating rate or the total integrated heat load. POST was then able to interpolate or extrapolate as necessary to find the heating rate at each time step throughout the trajectory. No constraint was placed on either the stagnation-point peak heating rate or the integrated heat load for the simulations in this study.

Entry Corridor and Heating Results

For the initial determination of entry corridor bounds and corridor widths, trajectory simulations were begun with due east, equatorial entries. The vehicle was targeted to an orbit with an apoapse altitude of 407 to 420 km. In this phase of the study, no targeting for final inclination was done. The corridor bounds are shown in Figure 2 as a function of entry velocity for both nominal and off-nominal atmospheric conditions. It is apparent that a constant percent increase or decrease in atmospheric density has little effect on the total entry corridor width. However, a density uncertainty of a given level will require the overshoot bound to be set using the low density limits and the undershoot boundary to be determined using the high density values; as shown in Figure 3, this results in a marked reduction of corridor width. Figures 4 and 5 illustrate the relatively modest sensitivity of the corridor width to changes of the ballistic coefficient from its nominal value of 25,500 kg/m^2; Figures 6 and 7 show that limiting the vehicle roll rate to 5 rather than 10 degrees per second has a minimal impact on the value of the undershoot bound or the entry corridor width. However, as should be expected, constraining the maximum vehicle deceleration to 3.5 rather than 5.0 G significantly restricts the undershoot bound and adversely effects the entry corridor width as illustrated in Figure 8. Figure 9 compares the corridors for the TransHab/Ellipsled and Apollo-derived vehicles for nominal atmospheric conditions and a 5 G deceleration limit; it is apparent that the higher lift-to-drag ratio of the TransHab/Ellipsled gives it a slight edge in terms of overall corridor width. Stagnation-point peak heating rates and integrated heat loads are shown in Figures 10 and 11 for a TransHab with the nominal ballistic coefficient flying in

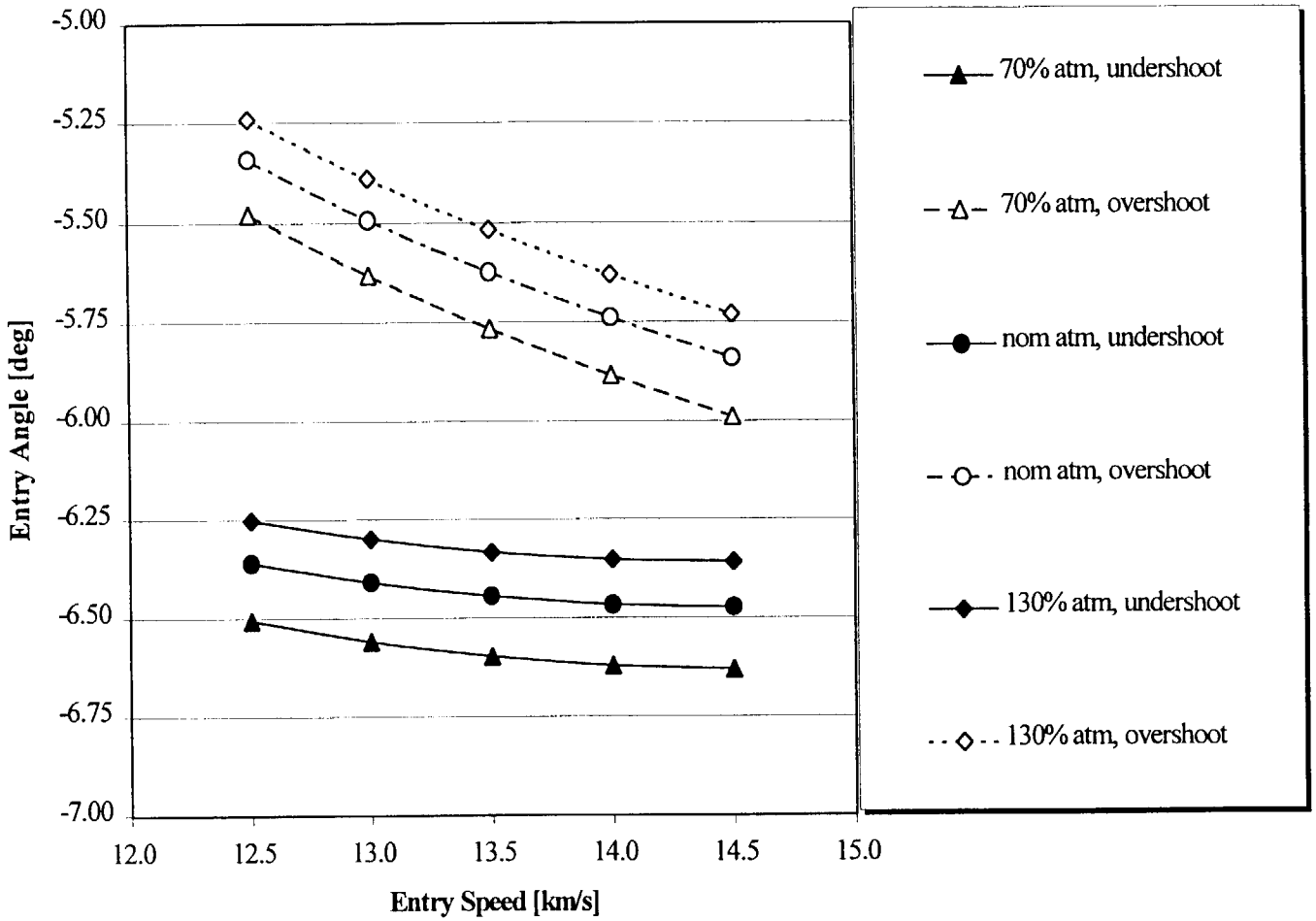

Figure 2. Corridor bounds as a function of entry velocity for various atmospheric densities

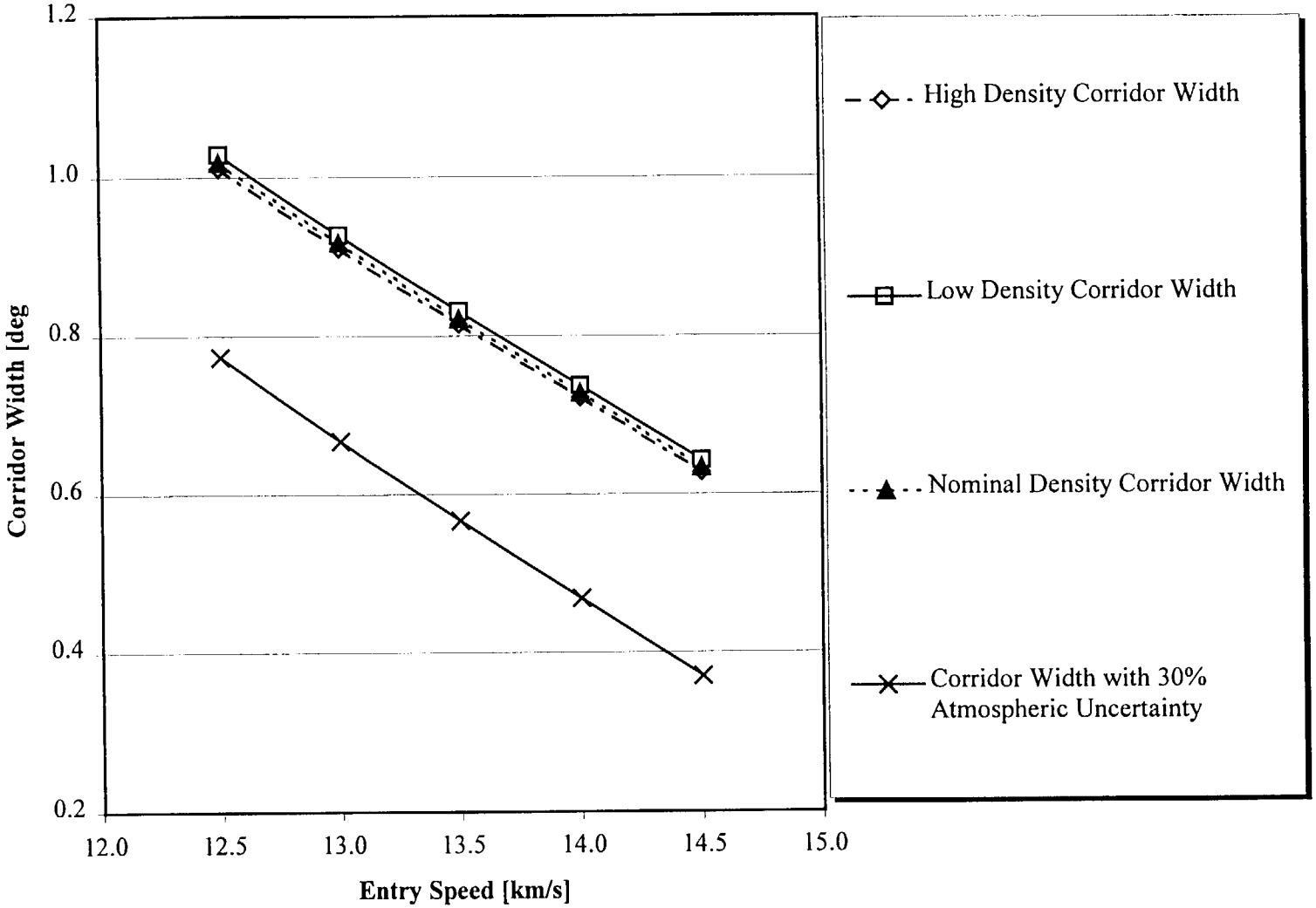

Figure 3. Corridor width as a function of entry velocity for various atmospheric density profiles

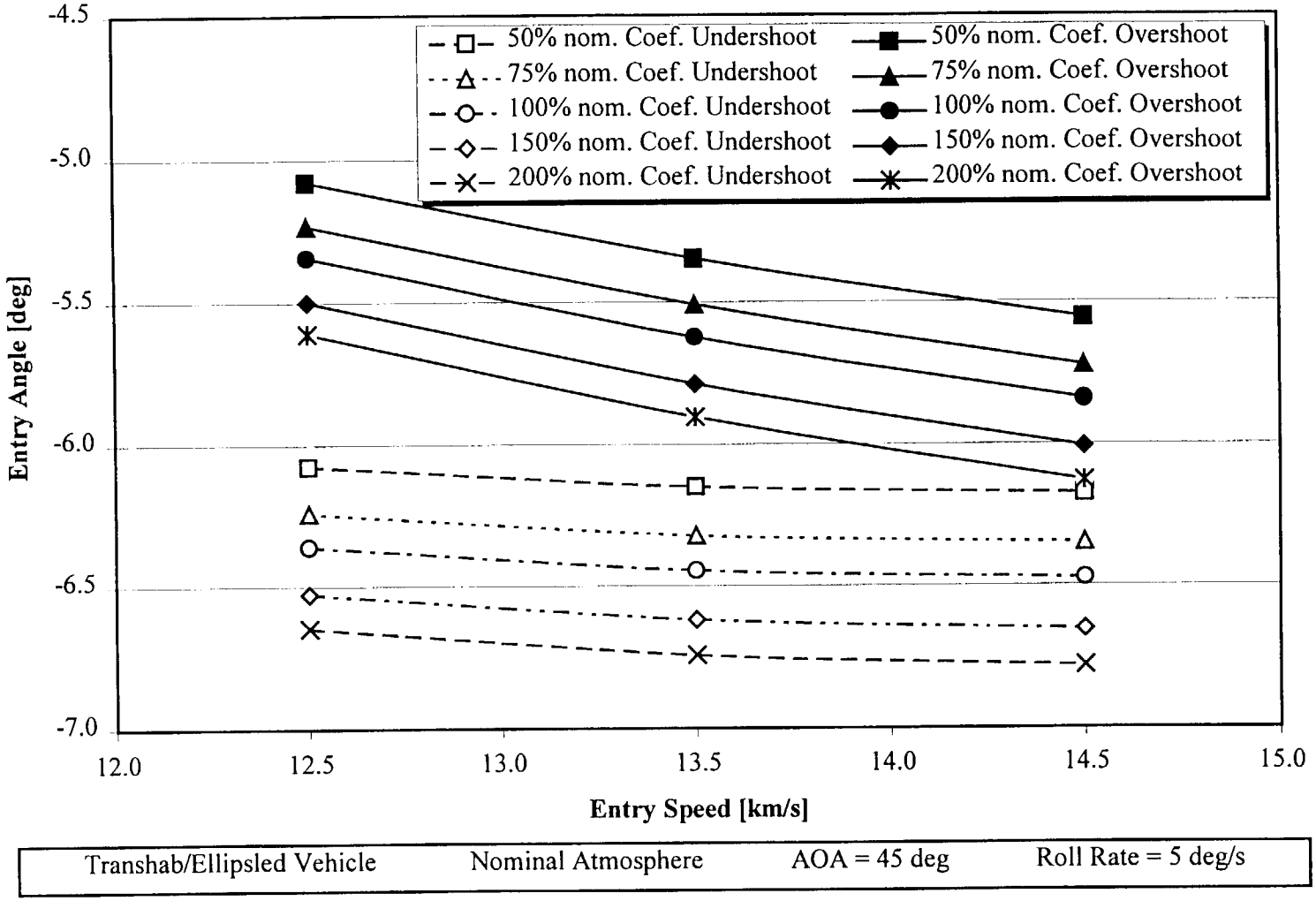

Figure 4. Corridor bounds as a function of entry velocity for various ballistic coefficients (nominal ballistic coefficient is 25,500 kg/m^2)

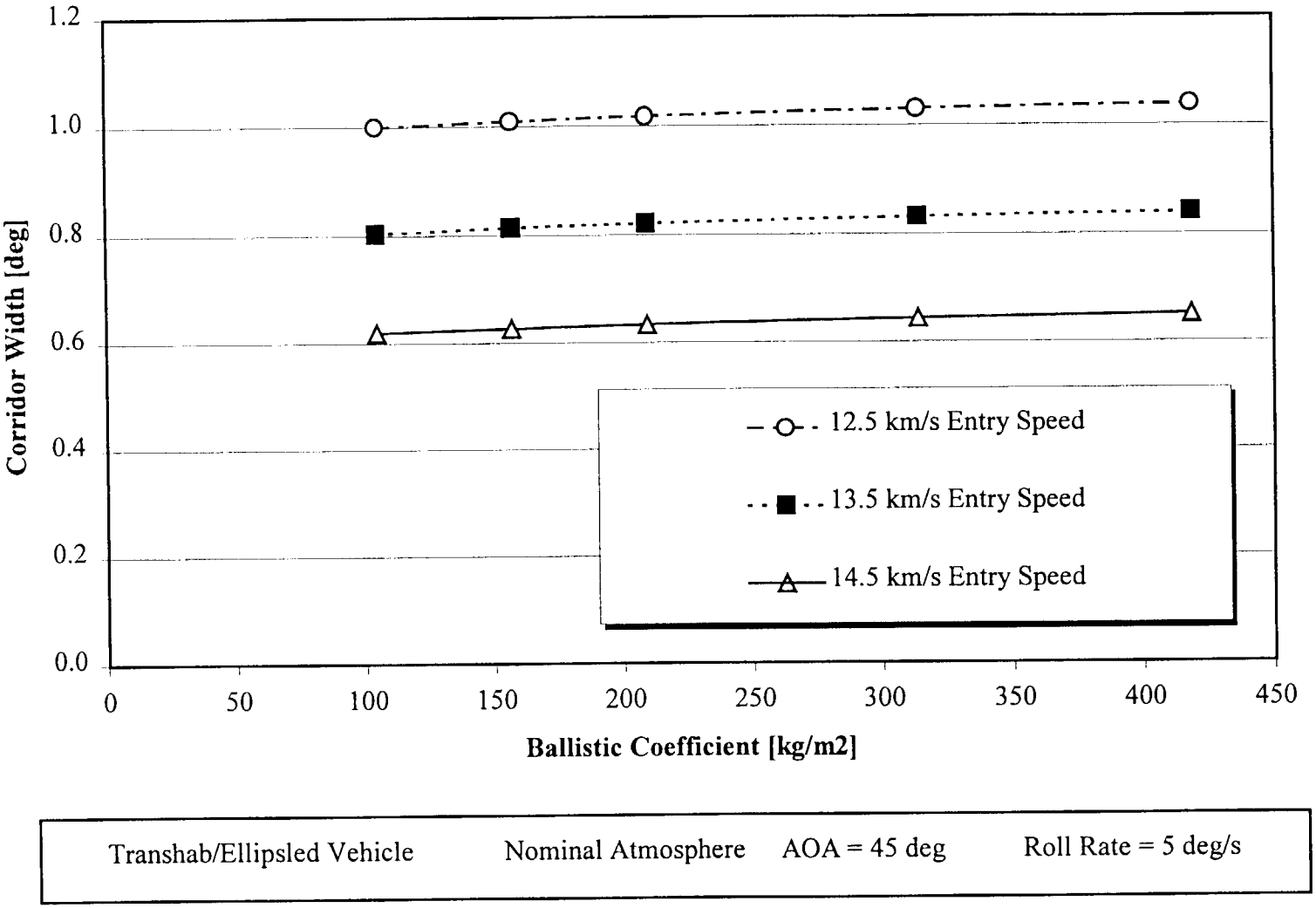

Figure 5. Entry corridor width as a function of vehicle ballistic coefficient

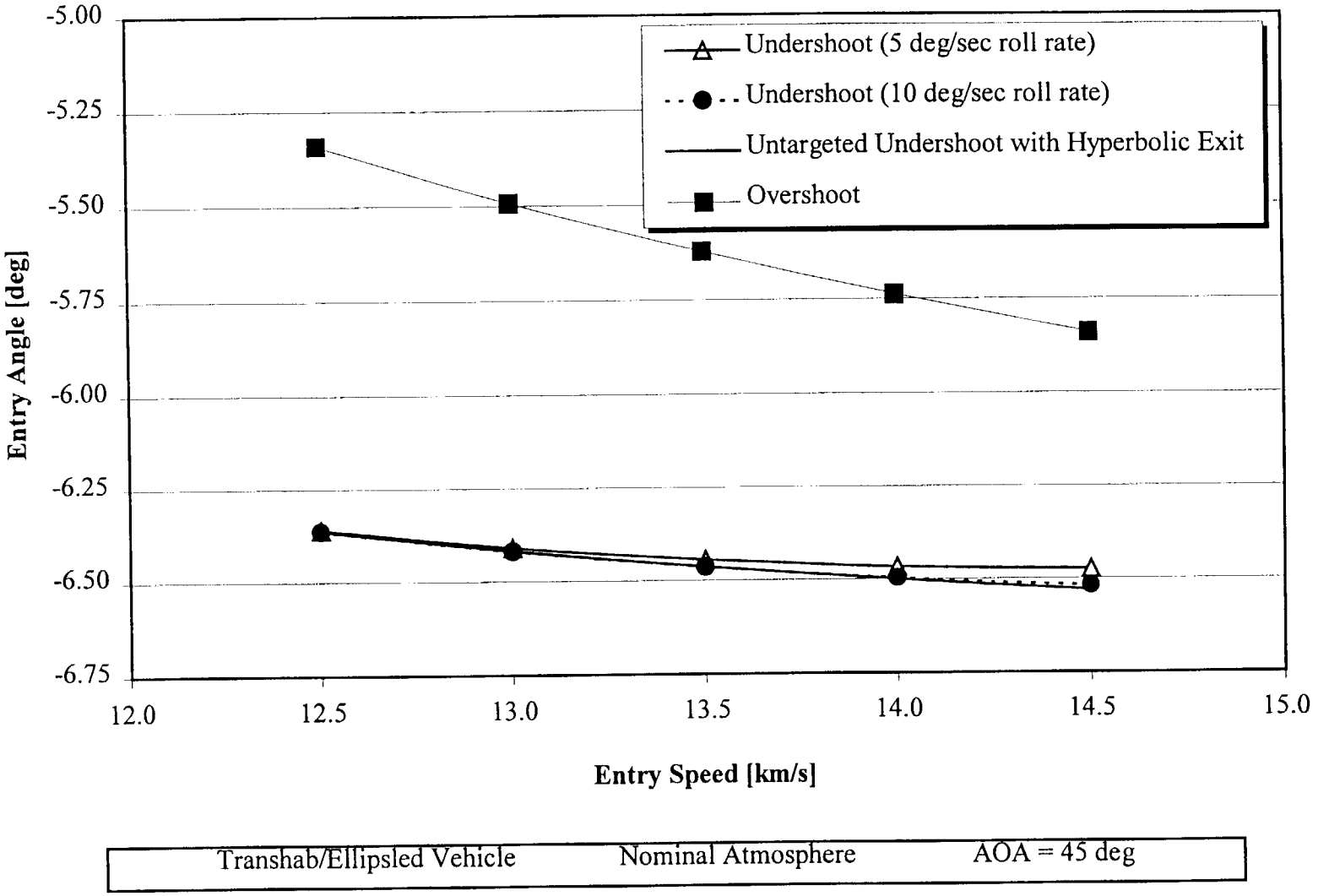

Figure 6. Corridor bounds for roll rates of 5 and 10 degrees per second

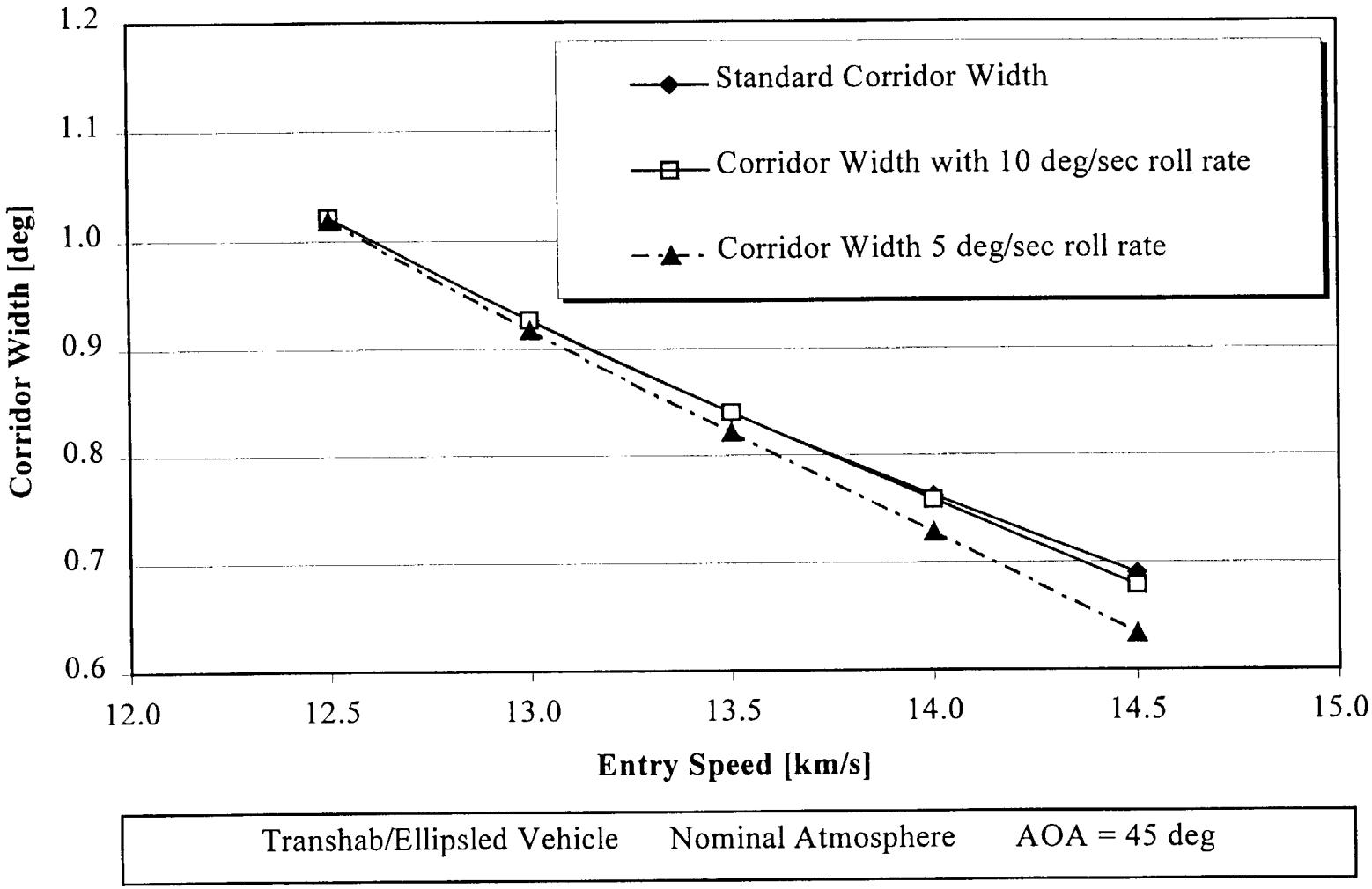

Figure 7. Entry corridor width for maximum roll rates of 5 and 10 degrees per second

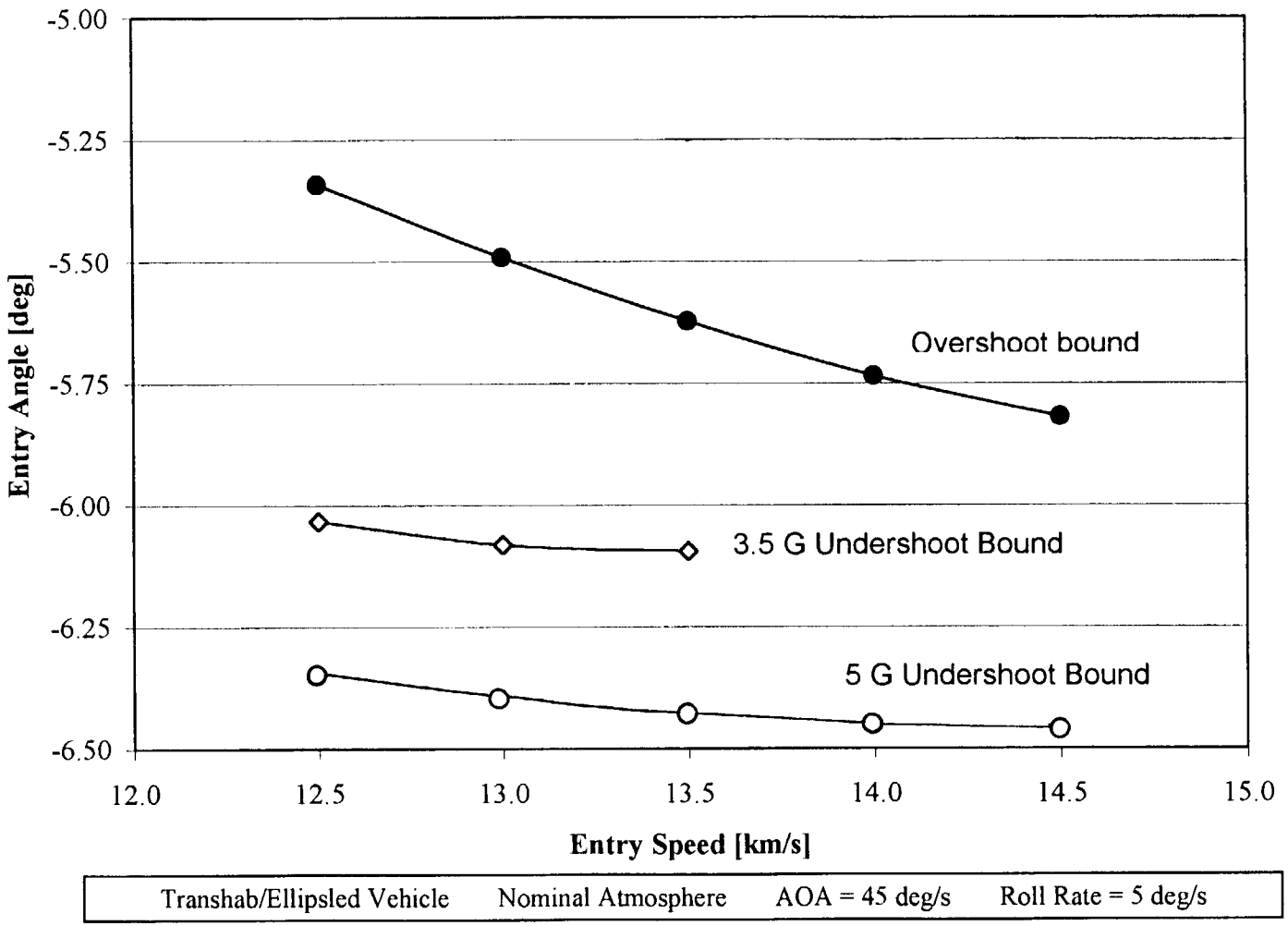

Figure 8. Corridor bounds as a function of entry velocity as for a 3.5 G deceleration limit

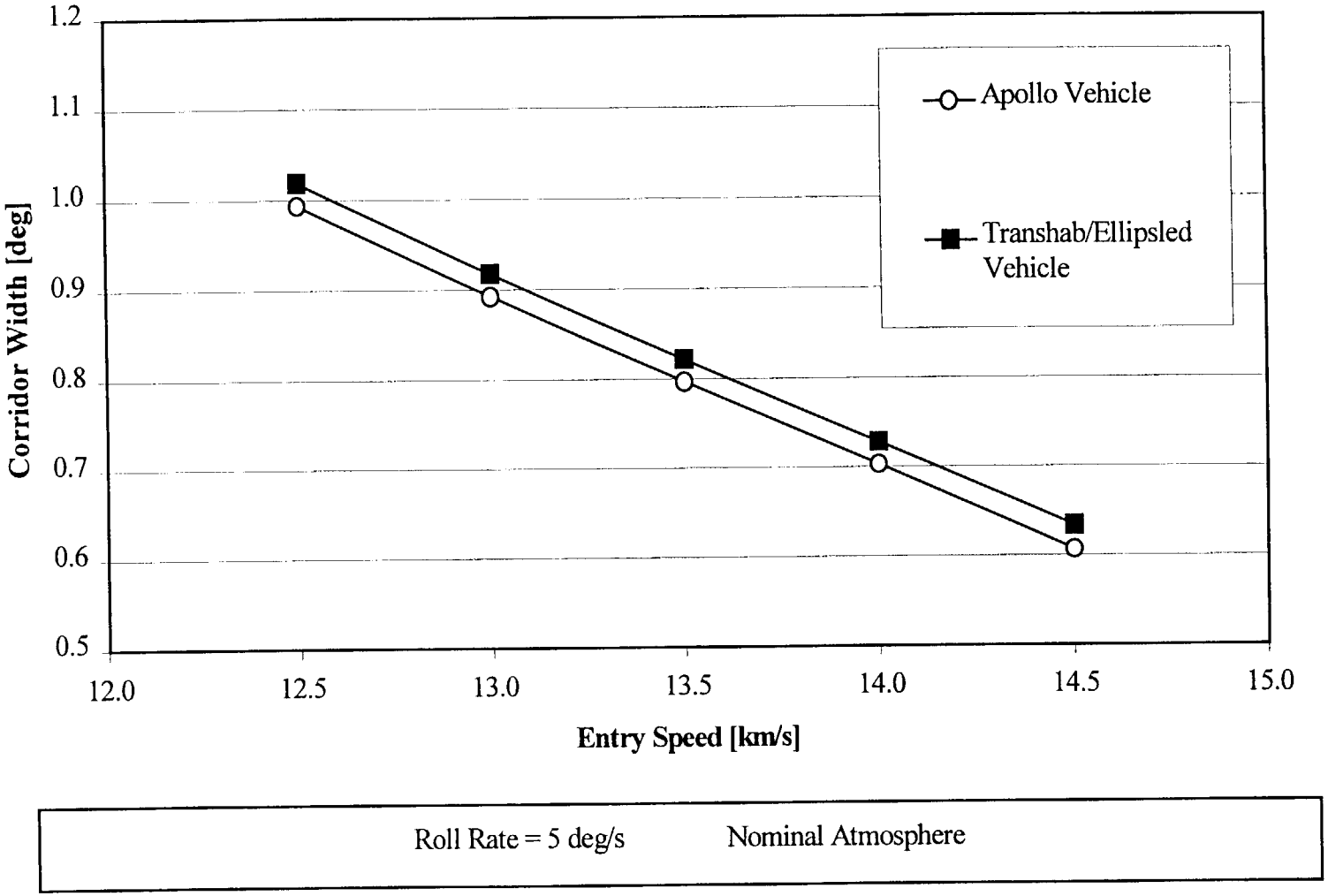

Figure 9. Corridor width of the TransHab/Ellipsled and Apollo-derived vehicles for nominal atmospheric density and a 5G deceleration limit

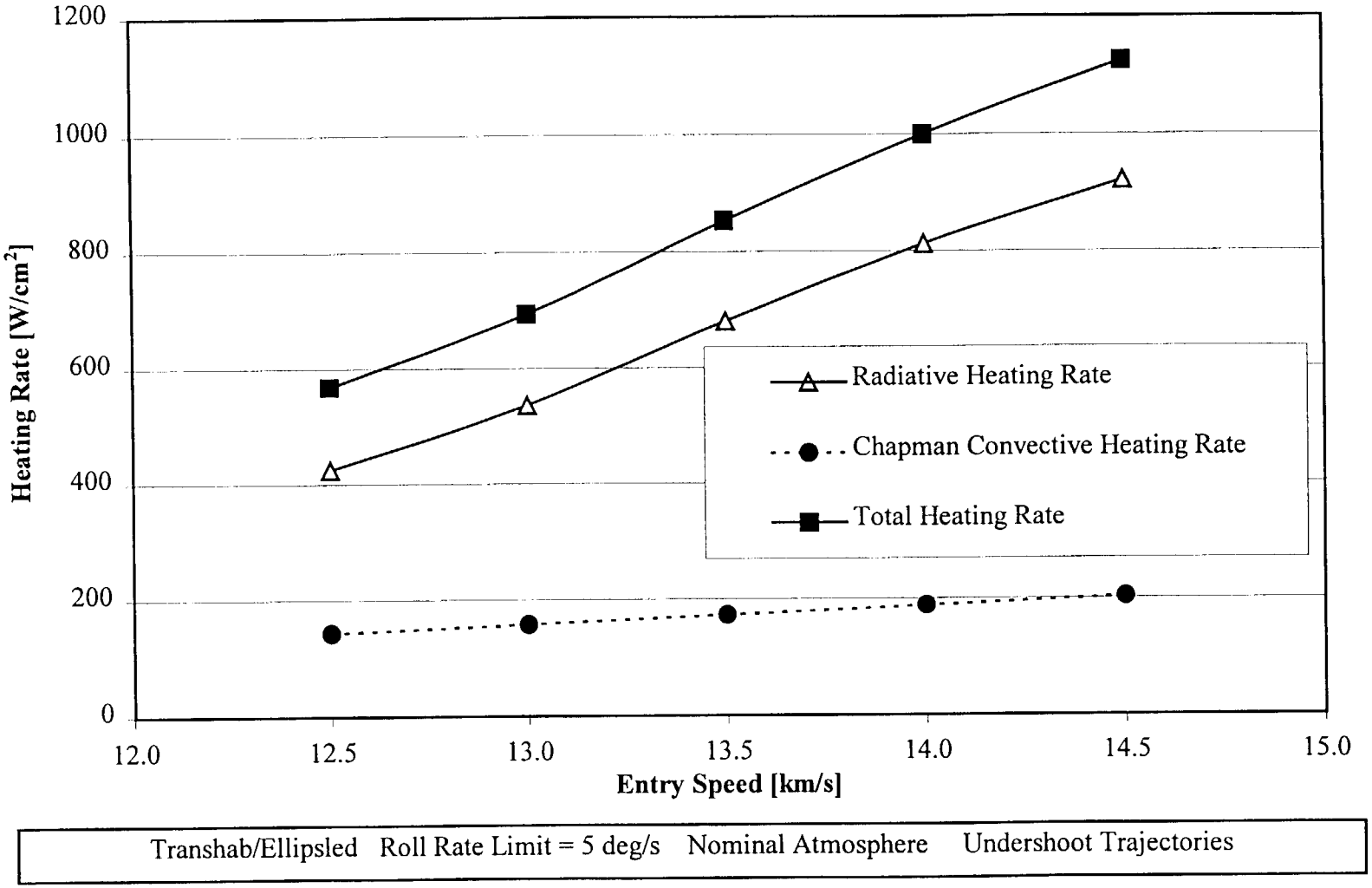

Figure 10. Stagnation-point peak heating rate for TransHab undershoot trajectories

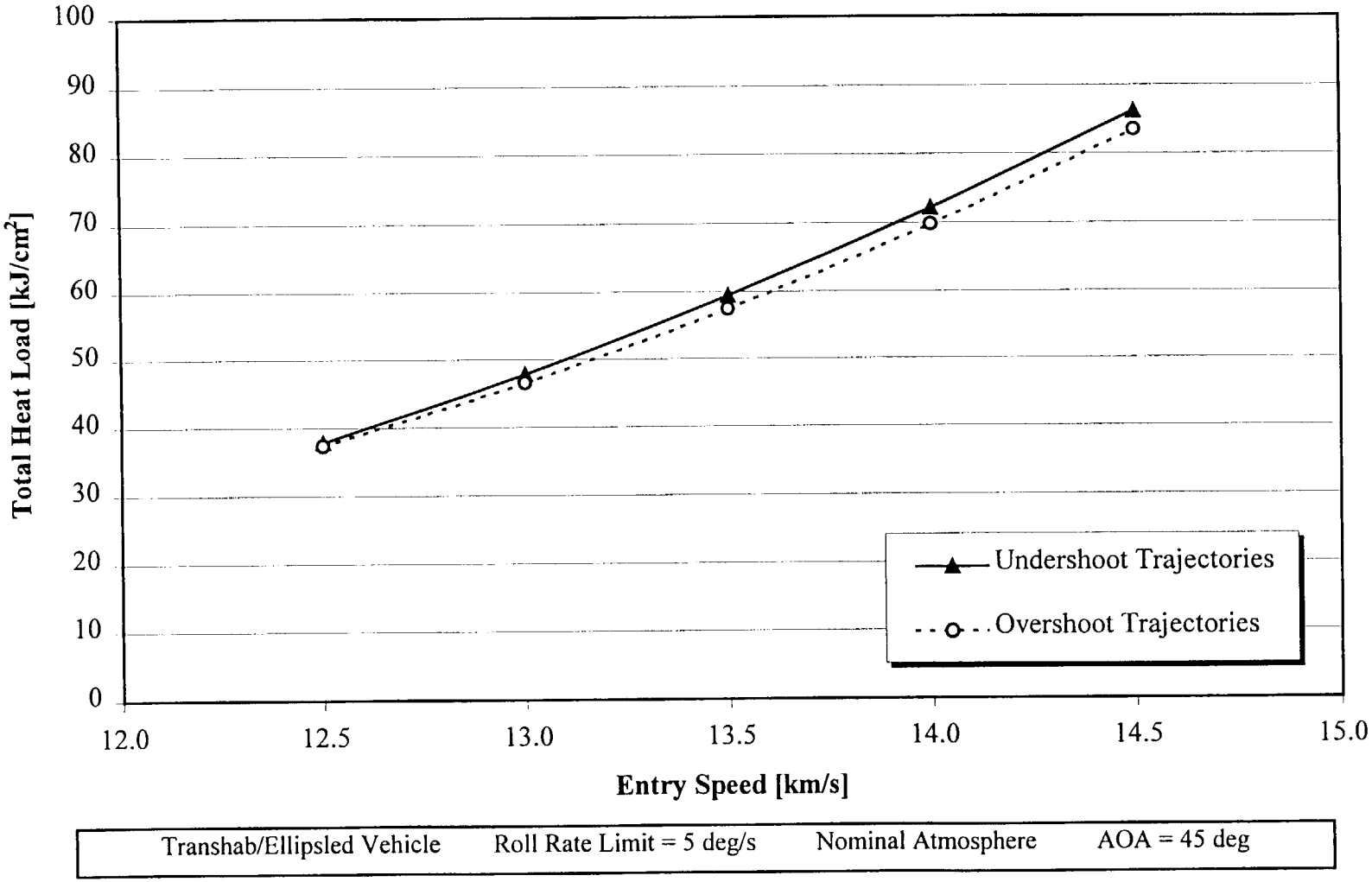

Figure 11. TransHab stagnation-point integrated heat load for Earth return aerocapture

standard atmospheric conditions. The variation of stagnation-point heating as a function of the vehicle ballistic coefficient is shown in Figures 12 and 13.

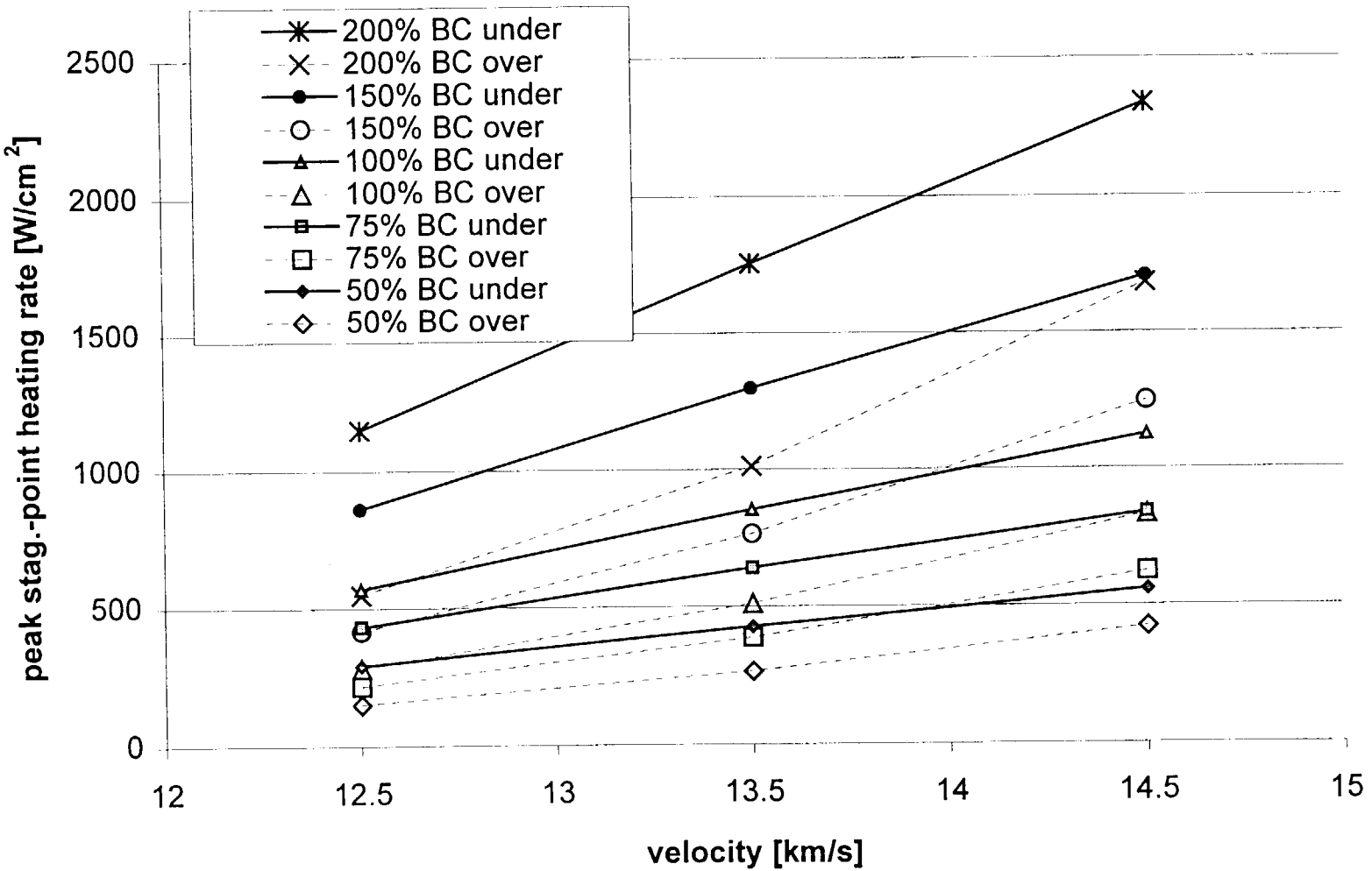

Figure 12. TransHab stagnation-point peak heating rate as a function of vehicle ballistic coefficient

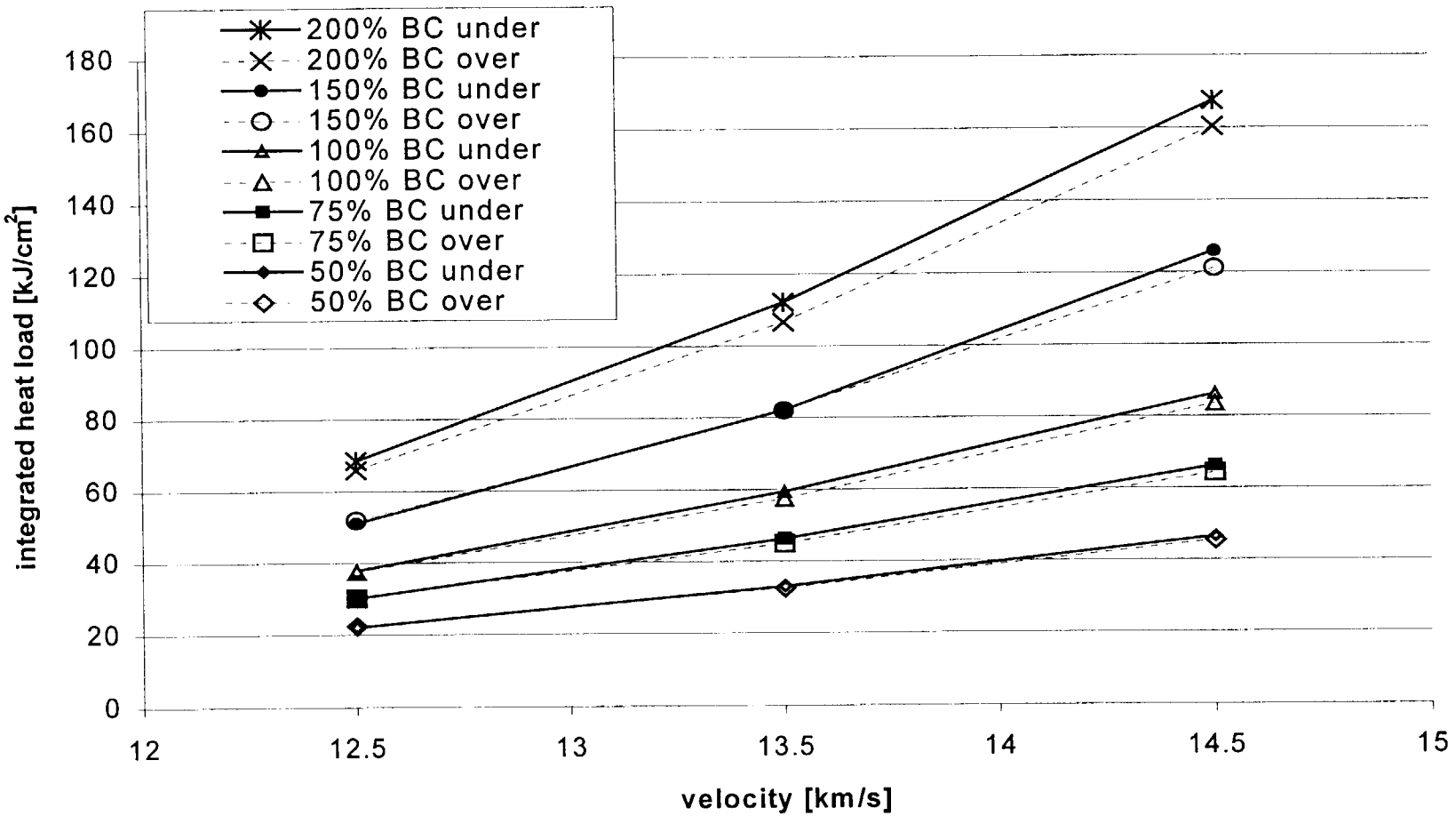

Figure 13. TransHab stagnation-point integrated heat load as a function of vehicle ballistic coefficient

Transitional & Free Molecular Flow Aerodynamic Coefficients

The data presented in this report thus far was based on vehicle aerodynamics calculated using modified Newtonian theory. However, Newtonian theory is only appropriate for determining continuum aerodynamic coefficients, and at altitudes above approximately 90 km, the freestream density is low enough that the continuum model is no longer valid. Viscous effects become increasingly important, and the coefficient of drag increases, while the coefficient of lift decreases. The change of the fluid flow regime from continuum to transitional and free molecular flow is based upon the Knudsen number.

Determination of the Knudsen Number

The Knudsen number (Kn) is defined by the ratio of the mean free path length, λ, to a characteristic length of the vehicle or body. According to the definition of the Knudsen number, the atmosphere can be roughly divided into three different layers: the continuum regime at relatively low altitudes, the free molecular flow area at the upper part of the atmosphere, and the transitional flow area in between. The boundaries of these layers are determined by certain values of the Knudsen number, which generally are set at $0.01<Kn<10$ for the transitional flow area. However, NASA used slightly different limits ($0.001<Kn<10$) for their studies of the Earth entry trajectory of the Stardust sample return capsule (Ref. 3). These altered limits were adopted for the present study as well. The characteristic length of the T/E configuration was 16.8 m, and the data for the mean free path length as a function of altitude was taken from the 1976 US Standard Atmosphere. The resulting flow regimes are shown in Figure 14.

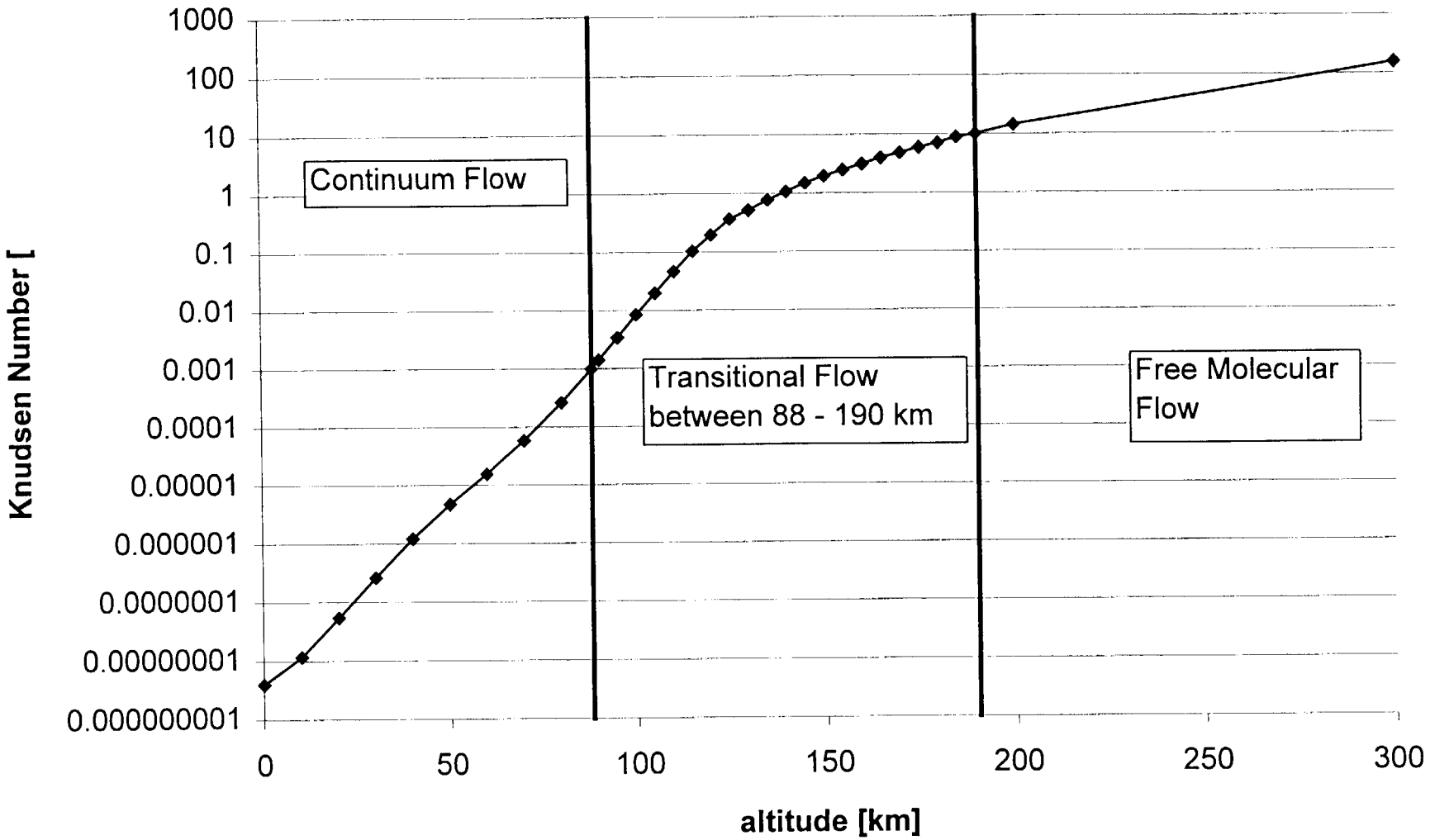

Figure 14. TransHab knudsen number as a function of altitude and aerodynamic flight regimes

Calculation of the Transitional Flow Aerodynamic Coefficients

The transitional flow aerodynamic coefficients were calculated with a bridging function described in Reference 3. Using free-molecular flow coefficients provided by Neil Cheatwood of the NASA Langley Research Center, the transitional aerodynamic coefficients presented in Figure 15 were determined for the TransHab/Ellipsled. These values are for an angle of attack of 45°, which corresponds to the trim angle for Mach numbers above 24. For a successful aerocapture, the Mach number will never drop below this level.

Effect on Entry Corridors of Transitional/Free Molecular Aerodynamics

Using the newly calculated aerodynamic coefficients, several simulations were run, and the results were compared with those obtained previously using only continuum flow aerodynamics. These simulations were done with the same basic settings as the previous runs with POST. The 1976 US Standard Atmosphere was used, and Earth modeled as an oblate spheroid; the initial flight azimuth was 90°, and the T/E flew the trajectory at an AOA of 45°. The same constraints were employed for the simulations, including the 5-g deceleration limit, the 407 km target apogee altitude and the maximum roll rate for the T/E of 5 deg/s. The bank angle modulation used to determine the undershoot boundaries was the single phase roll maneuver from 0° to 180°. However, the simulations were begun at an altitude of 200 km. Figure 16 shows a typical time history of C_D, C_L, the deceleration and the altitude for an undershoot trajectory. The constant values of the aerodynamic coefficients during the continuum flow (below an altitude of 88 km) and free molecular flow regimes (above 190 km) can be seen clearly.

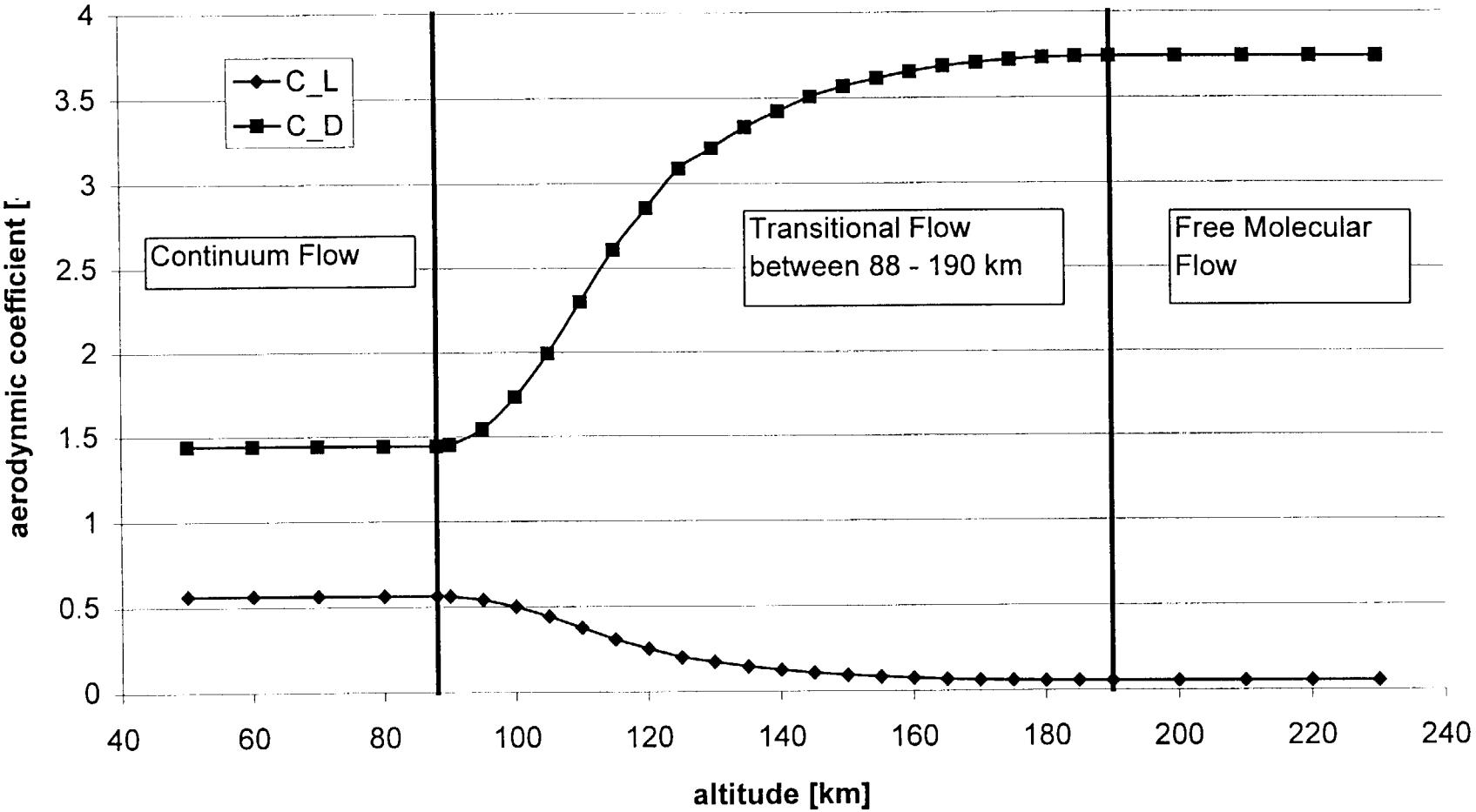

Figure 15. Aerodynamic force coefficients for the TransHab/Ellipsled as a function of altitude

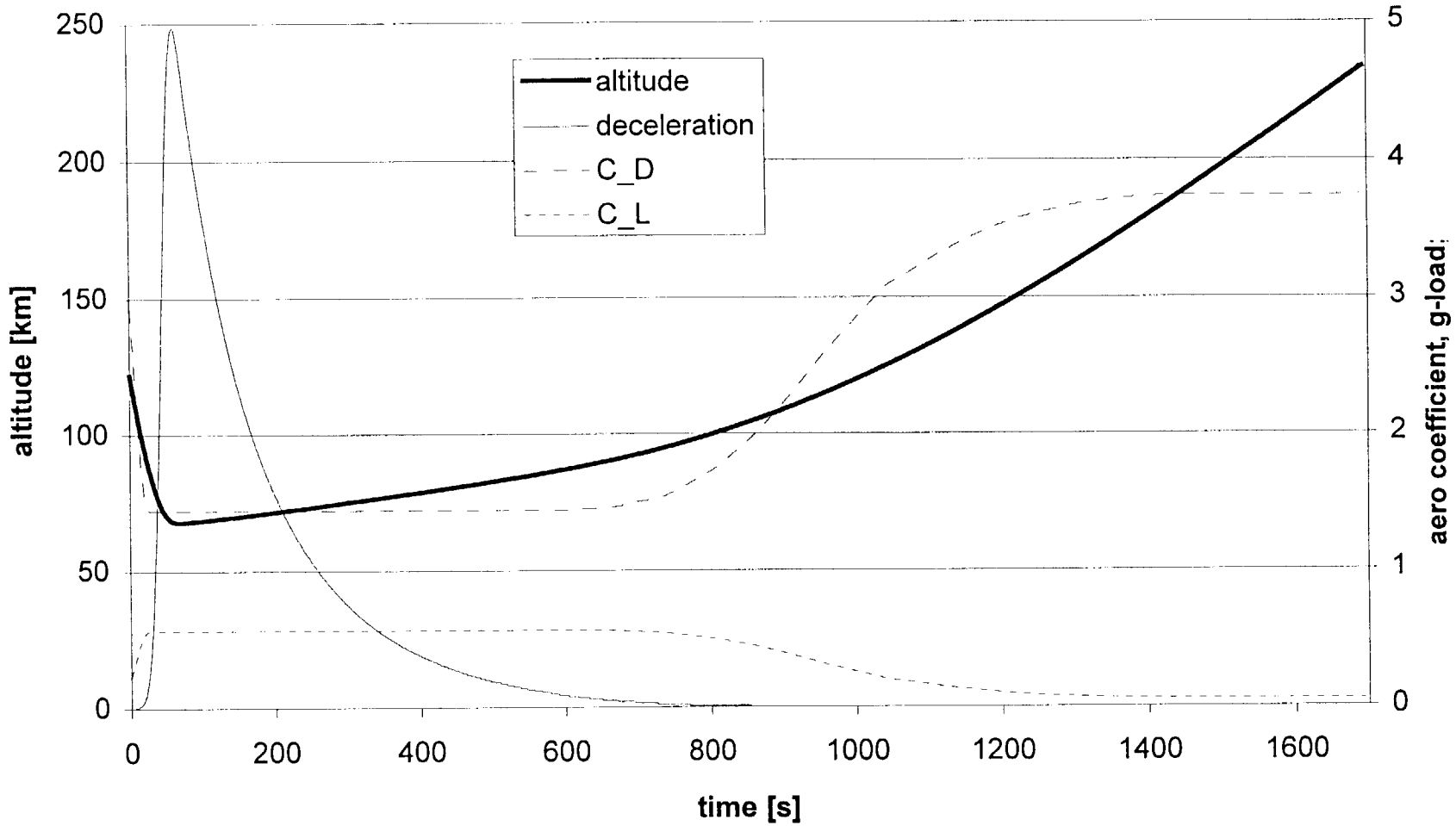

Figure 16. Variation of altitude, vehicle deceleration and force coefficients for the undershoot trajectory for a 14.5 km/s entry using a 5 deg/s maximum roll rate

The deceleration reached its maximum value early in the trajectory when the T/E flew through the denser parts of the atmosphere at low altitudes. Once differences which resulted from beginning the trajectory simulations at different altitudes were considered, the corridors determined using free molecular and transitional aerodynamics were virtually indistinguishable from those found using only continuum aerodynamics; corridor bounds for the two methods differed by approximately 0.01 degree.

.

Inclination Targeting & Minimization of the Post-Aerocapture ΔV

General Approach

After a vehicle executes an aerocapture maneuver, final orbital adjustments are required using a propulsive system. These primarily serve to raise the periapse altitude to its desired value and to correct the inclination to the target value. To obtain an adequate entry corridor width, bank angle modulation must be used for undershoot and mid-corridor trajectories. The turning trajectories which result can produce significant changes in the orbital inclination and increase the post-aerocapture ΔV required for inclination corrections. Increases in the post-aerocapture ΔV budget are not desirable since they result in higher mission mass and cost. A key to reducing the post-aerocapture ΔV is the minimization or elimination of inclination corrections. The inclination of the capture orbit can be targeted to a significant extent by small adjustments in the direction of the vehicle velocity vector in deep space; the roll control sequence during aerocapture typically will be required either to introduce no deviations in the final inclination of the orbital plane or to effect only modest corrections in the orbital inclination. This required the development of a new bank angle control strategy.

The previous bank angle modulation scheme began with a roll angle of 0° upon entry and executed a clockwise roll at a rate of 5 or 10 deg/s ending at 180°. During this maneuver, the lift-vector is always pointing to the same side of the vehicle; this causes a significant change in the orbital inclination. Directing the lift force first to one side of the vehicle and then to the other would decrease this effect. Many different options were examined, and a three-phase roll sequence was adopted. In this scheme, POST could

select start and end times for three roll phases during the trajectory. To add more flexibility, POST could also pick the initial bank angle at the time of atmospheric entry and the roll-rate with which each turn was executed, up to a maximum rate of 5 deg/s. An example of this bank angle modulation scheme is shown in Figure 17 for five different entry velocities and a target orbit with an inclination of 51.6°.

In most parts of this study, it was assumed that it was possible to pick the initial latitude of the atmospheric entry at Earth by performing a propulsive maneuver while on the interplanetary trajectory. (The propellant needed for this maneuver would be very low, since far away from Earth a small change in the flight path angle would result in a large change in the location of entry.) However, the azimuth of the trajectory was still assumed to be 90° upon reentry. Thus, a specific final orbital inclination could be targeted by selecting the latitude of entry to be close to the desired inclination and the entry azimuth to be 90° (due East). Although variations in the interplanetary arrival vector make this assumption of due east entries at selected latitudes unrealistic, this will have a negligible effect on the entry corridor widths and vehicle heating rates considered earlier in the study. Moreover, internally consistent entry latitude/azimuth combinations are not required for the development of roll control strategies intended to decrease or eliminate inclination changes during aerocapture and thereby minimize the post-aerocapture ΔV. It is shown later in this report that these same roll control strategies are successful when actual latitude/azimuth entry combinations are used.

Many trajectory simulations for this study targeted a parking orbit with an inclination of 0°. It was eventually realized that this is the most difficult inclination to

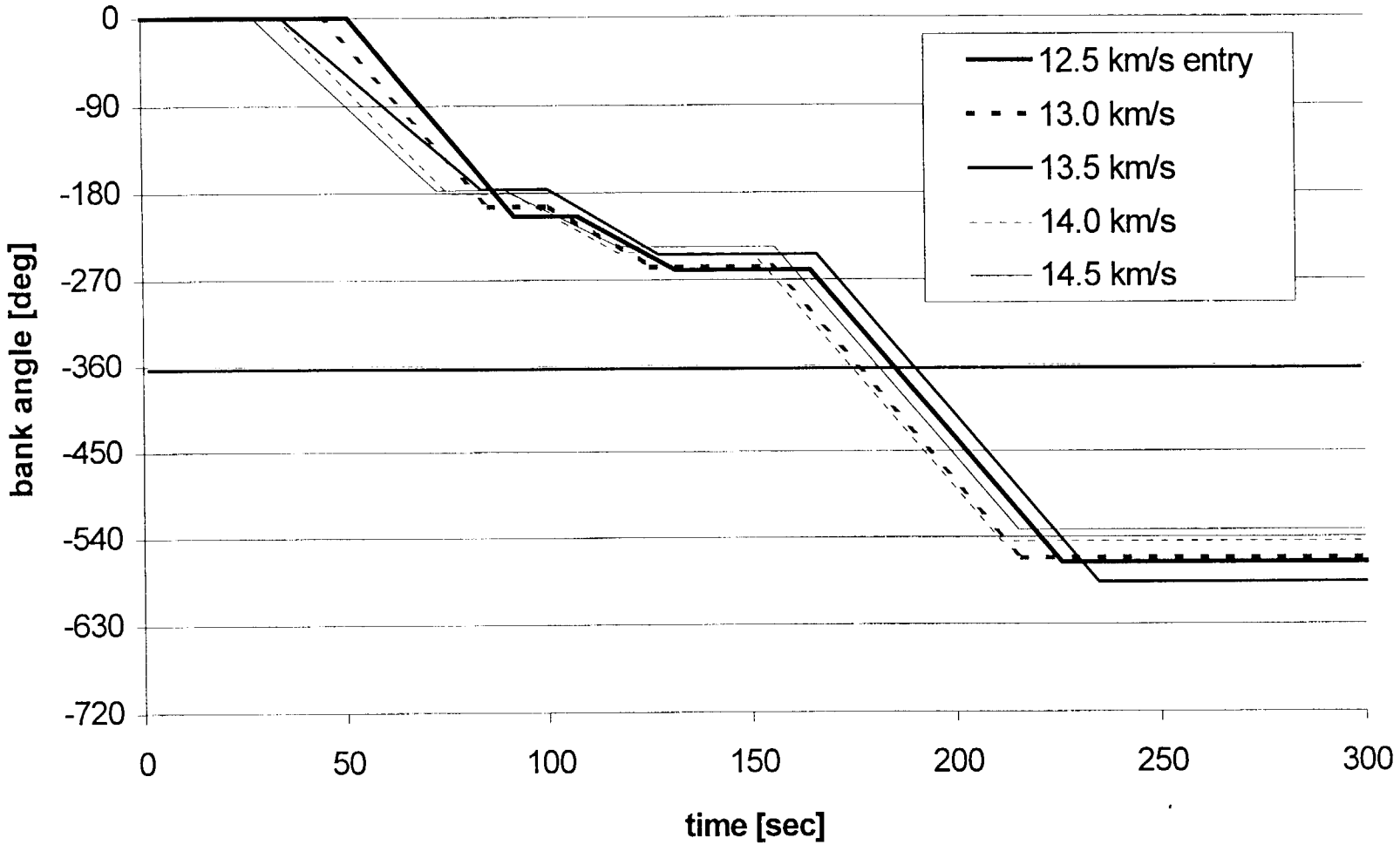

Figure 17. Bank angle sequences for minimization of post-aerocapture delta-V for a target inclination of 51.6 degrees

achieve. Figures 18 and 19 show why this is the case. They show a two dimensional view of a part of one hemisphere of the Earth.

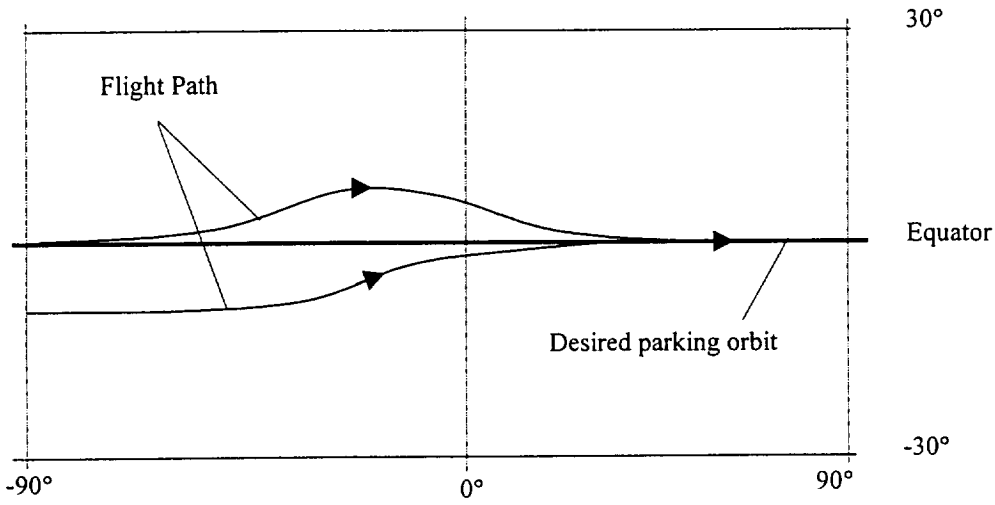

Figure 18. Desired parking orbit with an inclination of 0 degrees

If the desired parking orbit lies in the equatorial plane, as in Figure 18, the entry latitude of the vehicle must be fairly close to the equator, depending on the aerodynamic capabilities of the vehicle. Moreover, the vehicle must *exit* the atmosphere at a latitude of 0° with a due East azimuth (the velocity vector at exit is constrained both to a specific latitude and a specific azimuth). However, if the desired parking orbit has a target inclination greater than 0° - say, for example, 30 degrees - the vehicle can exit the atmosphere at any latitude between plus and minus 30 degrees, and an exit azimuth can be chosen which will place the vehicle in the desired parking orbit. As a result, there are fewer constraints on the exit conditions, and successful targeting is simplified.

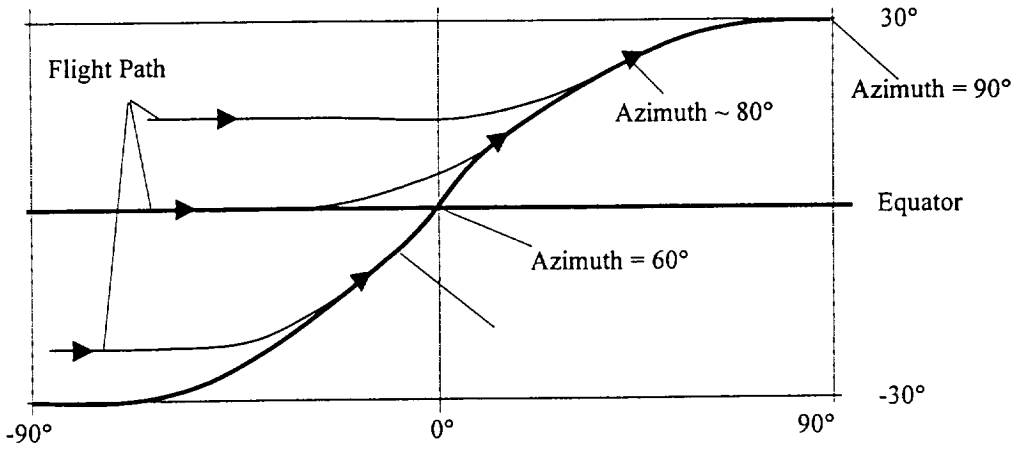

Figure 19. Desired parking orbit with an inclination 30 degrees

Trajectory Simulations for Various Target Inclinations

With the exception of the entry latitude, all simulations for this phase were done with the same settings used earlier in the study. The atmosphere was modeled by the 1976 US Standard Atmosphere, simulations began at an entry altitude of 121,900 m, and Earth was modeled as an oblate spheroid. The T/E flew with an angle-of-attack of 45°, and the entry velocities examined were 12.5, 13, 13.5, 14 and 14.5 km/s. The aerodynamic coefficients were determined using Modified Newtonian theory. As mentioned before, the azimuth upon entry was assumed to be 90°. In the interest of time, only entry angles for mid-corridor trajectories were examined in this phase of the study. The constraints for the trajectory were again the 5-g deceleration limit and the 407 km altitude of the apogee. Additionally, two new constraints were entered into the POST input deck. The first guaranteed that the bank angle turning rate could not exceed 5 deg/s, while the second one was an equality constraint that set the inclination of the target orbit.

Target Orbit with a 51.6° Inclination

The first target inclination examined was 51.6°, which corresponds to that one of the International Space Station. Since the T/E configuration is not intended to be used for a direct entry trajectory or surface descent, the crew, their research results and the Martian samples will have to be transferred to another vehicle for descent to Earth's surface. If, for some reason, the use of the Mars Ascent Vehicle as a surface return capsule is not possible, a potential strategy for crew retrieval would be to rendezvous with a small crew taxi or the ISS. It is also conceivable that a rendezvous with the ISS could be required as a contingency plan in the unlikely event that the crew required quarantine prior to descent to the surface. Moreover, capture into a 51.6° orbit would facilitate the use of a Russian retrieval system.

The simulations for the case with a target inclination of 51.6° were run with an entry latitude of 50.6° and an entry azimuth of 90°. The data determined for the bank angle modulation sequence and the exit orbit parameters are presented in Table 3. (The roll control sequence for this case is shown graphically in Figure 17.) The turning rate of the T/E is negative because the initial latitude is smaller than the target inclination. As a result, the vehicle had to perform a slight turn to the left, which could only be accomplished by a counterclockwise turn when you look from behind the T/E along its trajectory. This turn direction is negative by definition. The altitude of the exit perigee is also negative, i.e. below the surface. Therefore, the T/E has to perform a correction burn at apoapse to raise the perigee altitude. It is obvious from Table 3 that POST did not need to adjust the initial bank angle to target the desired parking orbit. Note that the turn maneuver was initiated earlier with higher entry velocities. This is because the T/E has to

stay in the atmosphere longer in order to dissipate enough energy to reach the desired parking orbit. The data given under the column 'time to 407 km' is the time needed by the T/E to reach an altitude of 407 km along the aerocapture trajectory. These results indicate that capture into a target orbit with an inclination of 51.6 may be feasible.

entry velocity [km/sec]	entry angle [deg]	init. bank angle [deg]	$T1_{roll\_start}$ [sec]	TR1 (turn rate) [deg/sec]	$T1ST_{roll\_stop}$ [sec]
12.5	-5.851	0.000	50.867	-4.965	41.097
13	-5.950	0.000	44.345	-4.687	41.395
13.5	-6.034	0.000	34.557	-3.586	49.095
14	-6.102	0.000	33.577	-4.301	42.041
14.5	-6.157	-0.001	27.409	-3.921	45.108

enrty velocity [km/sec]	$T2_{roll\_start}$ [sec]	TR2 (turn rate) [deg/sec]	$T2ST_{roll\_stop}$ [sec]	$T3_{roll\_start}$ [sec]	TR3 (turn rate) [deg/sec]	$T3ST_{roll\_stop}$ [sec]
12.5	15.417	-2.306	24.237	32.825	-5.000	61.243
13	14.996	-2.521	24.894	29.362	-5.000	60.979
13.5	16.669	-2.512	27.062	38.750	-5.000	68.556
14	15.786	-2.374	25.840	33.128	-5.000	60.503
14.5	17.246	-2.133	27.825	38.217	-5.000	59.271

entry velocity [km/sec]	peak deceleration [g]	time to 407km [sec]	inclination [deg]	period [min]	apogee altitude [km]	perigee altitude [km]
12.5	3.817	1969.228	51.603	88.405	413.406	-0.928
13	4.464	1992.070	51.597	88.219	410.262	-16.183
13.5	4.003	2093.221	51.600	88.318	408.276	-4.353
14	4.998	1973.563	51.601	88.205	410.606	-17.969
14.5	5.000	2073.693	51.597	88.215	408.142	-14.463

Table 3. Bank angle modulation and final orbital parameters for a parking orbit with a 51.6° target inclination

Target Orbit with a 28.5° Inclination

This orbital inclination was examined because it is consistent with the position of NASA Kennedy Space Center. The simulations were run with an entry latitude of 27.5° and a due east initial azimuth; data obtained for the bank angle modulation sequences and exit orbits are presented in Table 4. Again in this case, POST did not need to modify the entry bank angle to reach the desired parking orbit. The bank angle modulation sequence was very similar to that for the 51.6° target orbit, although the start of the third roll maneuver was approximately 45 seconds later for the 28.5° case. In addition, the perigee altitude was about 80 km higher.

entry velocity [km/sec]	entry angle [deg]	init. bank angle [deg]	$T1_{roll\_start}$ [sec]	TR1 (turn rate) [deg/sec]	$T1ST_{roll\_stop}$ [sec]
12.5	-5.851	0.001	52.015	-4.878	38.536
13	-5.950	0.000	43.302	-4.156	48.674
13.5	-6.034	-0.001	37.140	-4.034	51.168
14	-6.102	-0.002	30.744	-3.744	54.093
14.5	-6.157	-0.009	16.213	-2.693	72.256

entry velocity [km/sec]	$T2_{roll\_start}$ [sec]	TR2 (turn rate) [deg/sec]	$T2ST_{roll\_stop}$ [sec]	$T3_{roll\_start}$ [sec]	TR3 (turn rate) [deg/sec]	$T3ST_{roll\_stop}$ [sec]
12.5	19.546	-2.624	17.030	80.117	-5.000	63.846
13	20.577	-0.703	29.492	61.860	-5.000	68.156
13.5	21.037	-0.702	31.743	60.046	-5.000	57.512
14	21.182	-0.627	32.847	63.459	-5.000	59.519
14.5	15.140	-0.878	28.053	77.599	-5.000	63.014

entry velocity [km/sec]	peak deceleration [g]	time to 407km [sec]	inclination [deg]	period [min]	apogee altitude [km]	perigee altitude [km]
12.5	2.944	2455.415	28.502	89.182	413.899	75.574
13	3.237	2399.275	28.501	89.202	415.896	75.595
13.5	3.619	2377.226	28.487	89.118	414.474	68.637
14	3.938	2416.970	28.489	89.134	413.961	70.731
14.5	4.315	2402.572	28.503	89.202	415.959	75.520

Table 4. Bank angle modulation and final orbital parameters for a parking orbit with a 28.5° target inclination

Target Orbit with a 5.3° Inclination

Europe's spaceport is located in Korou, French Guyana in South America. With a latitude of 5.3°, it is very close to the equator and has the advantage compared to the other launch locations that a smaller rocket could be employed to lift a crew return vehicle into LEO. At the moment, the Ariane 5 launcher is capable of lifting 18 tons into LEO, and this capability is expected to improve over the next few years. This lift capacity would be sufficient for a crew return vehicle without the necessity of developing a new launch system.

entry velocity [km/sec]	entry angle [deg]	init. latitude [deg]	init. bank angle [deg]	$T1_{roll\_start}$ [sec]	TR1 (turn rate) [deg/sec]	$T1ST_{roll\_stop}$ [sec]
12.5	-5.851	5.210	0.000	50.245	-4.495	37.708
13	-5.950	3.591	0.000	43.594	-4.596	40.695
13.5	-6.034	3.336	0.000	37.650	-4.448	40.749
14	-6.102	3.469	0.000	31.843	-4.111	42.414
14.5	-6.157	3.364	0.000	25.378	-3.761	45.542

entry velocity [km/sec]	$T2_{roll\_start}$ [sec]	TR2 (turn rate) [deg/sec]	$T2ST_{roll\_stop}$ [sec]	$T3_{roll\_start}$ [sec]	TR3 (turn rate) [deg/sec]	$T3ST_{roll\_stop}$ [sec]
12.5	15.457	-2.023	22.829	34.751	-5.000	59.236
13	15.064	-2.505	24.937	29.644	-5.001	60.990
13.5	14.492	-2.670	24.937	28.283	-5.000	61.353
14	15.823	-2.444	26.600	34.285	-5.000	59.986
14.5	17.114	-2.288	28.497	39.295	-5.000	57.897

entry velocity [km/sec]	peak deceleration [g]	time to 407km [sec]	inclination [deg]	period [min]	apogee altitude [km]	perigee altitude [km]
12.5	3.258	2257.772	5.300	89.287	421.826	78.014
13	4.257	2119.825	5.303	88.806	417.760	34.470
13.5	5.007	1991.367	5.297	88.578	418.217	11.397
14	4.995	1957.429	5.298	88.730	421.312	23.441
14.5	5.000	2075.383	5.296	88.686	417.769	22.567

Table 5. Bank angle modulation and final orbital parameters for a parking orbit with a 5.3° target inclination

Table 5 presents the results of simulations targeting an orbit with an inclination of 5.3°. It was not possible to reach the desired orbit using a fixed entry latitude and a due east entry azimuth. Therefore, the geocentric latitude was entered as an additional control in the POST input deck. Except for this difference, the data presented in Table 5 is very similar to that for the previous cases.

The bank angle modulations and final orbital parameters shown in Tables 3 through 5 indicate that a roll control strategy has been developed which is able to minimize inclination changes during aerocapture and target parking orbits with specific inclinations, thereby decreasing post-aerocapture ΔV requirements.

High Elliptical Parking Orbit

The examination of this special parking orbit was motivated by two facts; first, a higher, more energetic target orbit would require the dissipation of less energy during the aerocapture and therefore, would lighten the vehicle's thermal protection system. Second, if the TransHab module is to be reused on a subsequent outbound Mars trajectory, a higher parking orbit would result in a lower trans-Mars injection ΔV. Moreover, NASA has considered the use of a high altitude, circular parking orbit prior to the trans-Mars injection (Ref. 4). In this scenario, the interplanetary vehicle would be spiraled to this 120,000 km orbit using a solar sail or electric propulsion system. A dedicated upper stage could rendezvous with the T/E in its elliptical target orbit and boost it into the high altitude circular orbit for mating with the rest of the interplanetary vehicle. Table 6 shows the results of an aerocapture to a 407 x 120,000 km orbit with an inclination of 28.5 degrees.

The simulations for the entry velocities 13.5, 14 and 14.5 km/s were run with an entry latitude of 27.5° and due east initial azimuth. However, it was not possible to target the desired parking orbit using this fixed entry latitude for the lower velocities of 12.5 and 13 km/s. Therefore, for these cases, the initial geocentric latitude was entered as additional control in the POST input deck. As in the previous cases, POST did not need to adjust the entry bank angle to target the desired parking orbit. Thus, for this simulation, the initial bank angle control was deleted in the POST input deck.

entry velocity [km/sec]	entry angle [deg]	init. latitude [deg]	$T1_{roll\_start}$ [sec]	TR1 (turn rate) [deg/sec]	$T1ST_{roll\_stop}$ [sec]
12.5	-5.767	28.472	4.888	-5.068	56.774
13	-5.508	28.462	4.541	-3.634	21.840
13.5	-5.762	27.500	7.801	-5.094	21.803
14	-5.961	27.500	17.609	-4.037	25.192
14.5	-6.079	27.500	25.697	-4.817	27.270

entry velocity [km/sec]	$T2_{roll\_start}$ [sec]	TR2 (turn rate) [deg/sec]	$T2ST_{roll\_stop}$ [sec]	$T3_{roll\_start}$ [sec]	TR3 (turn rate) [deg/sec]	$T3ST_{roll\_stop}$ [sec]
12.5	4.853	-4.310	9.269	4.782	-5.068	31.579
13	4.541	-5.000	7.305	4.509	-4.100	16.408
13.5	4.159	-2.310	7.176	4.160	-5.093	22.509
14	4.782	-4.811	7.467	4.791	-5.000	23.754
14.5	4.977	-5.000	7.588	5.059	-3.277	24.524

entry velocity [km/sec]	peak deceleration [g]	time to 407km [sec]	inclination [deg]	period [min]	apogee altitude [km]	perigee altitude [km]
12.5	3.973	345.655	28.500	2837.202	119969.297	71.010
13	2.573	424.846	28.500	2838.521	119999.052	82.422
13.5	3.981	394.598	28.500	2837.264	119964.218	78.024
14	5.000	384.342	28.500	2837.874	119986.415	74.860
14.5	5.000	396.461	28.500	2838.596	120007.633	76.169

Table 6. Bank angle modulation and final orbital parameters for a high elliptical parking orbit with a 28.5° target inclination

The use of the capsule from the Mars Ascent Vehicle for the crew descent to Earth's surface would eliminate the need for a transfer taxi to rendezvous with the T/E in this high-energy, elliptical orbit. It must be realized that the potential benefits afforded by aerocapture into a high-energy, elliptical orbit may be offset to some degree by the added complexity of aligning the capture orbit with the departure hyperbola for the next trans-Mars injection. Nevertheless, the data in Table 6 indicates that capture into such a highly elliptical orbit may be feasible.

Post-Aerocapture ΔV Requirements

Once the parameters of the capture orbits were determined using POST, it was possible to calculate the post-aerocapture ΔV and the propellant needs to place the T/E in the desired parking orbits. The resulting data is presented in Figure 20, where the post-aerocapture ΔV is shown as a function of the entry vehicle velocity. NASA has budgeted a ΔV of 230 m/s for final orbital adjustments into a 407 km orbit. Using the proposed propulsion system with a specific impulse of 375 s, this corresponds to 1546 kg of propellant. It is apparent that the post-aerocapture ΔV is not strongly dependent on entry velocity. The ΔV for the undershoot trajectory exceeds the level set by NASA by nearly 100 m/s, primarily because it used a single-phase roll maneuver without an attempt to target a specific inclination. With the exception of the overshoot case, the other simulations used a three-roll sequence targeted to a specific inclination, and all were well within the proposed ΔV budget. The differences in the values for the various curves are primarily due to the variations in the post-aerocapture perigee altitude. The high-energy, elliptical parking orbit required very little energy to raise the periapse altitude and as a

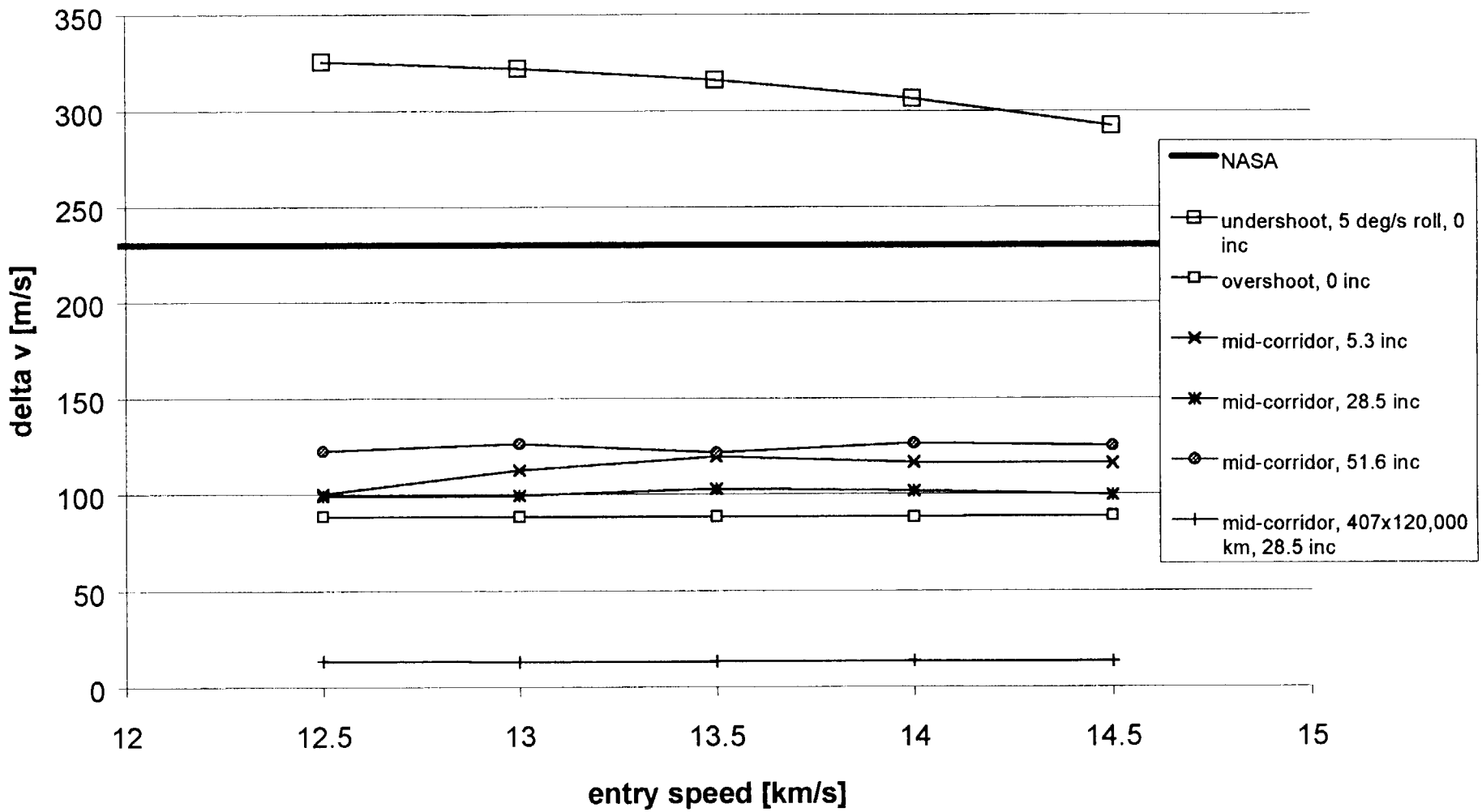

Figure 20. Post-aerocapture Delta V for the TransHab/Ellipsled to reach a 407 km circular orbit

result, had a lower total ΔV than the other cases. Of course, atmospheric and aerodynamic dispersions would be expected to decrease the targeting accuracy and raise the post-aerocapture ΔV above the nominal values shown in Figure 20 for all cases considered.

Entry State Coming from an Interplanetary Trajectory

The entry vector of the T/E for all simulations described thus far in this report was described by six variables; the first three, entry velocity, entry angle and the azimuth of the velocity vector define the direction and magnitude of the velocity. The other three variables, the longitude, the geocentric latitude and the geodetic altitude define the initial position of the vehicle in the three-dimensional space with reference to the middle of the Earth, the origin of the coordinate system. The azimuth of the velocity vector, the geocentric latitude, and the longitude had no special constraints, and so it was assumed that they could be chosen freely. However, this is not possible if the arrival conditions from a specific interplanetary transfer are considered, because the state vector at arrival may preclude certain combinations of entry latitude, longitude and azimuth. In order to target an orbit with a specific inclination realistically, it is necessary to start with the correct entry latitude/azimuth combination, and these values depend on the patch conditions at the edge of Earth's sphere of influence.

Representative interplanetary trajectory data specifying the arrival state for particular mission opportunities was provided by Larry Kos of NASA Marshall Space Flight Center. Declination, right ascension, arrival time and V_∞ at the edge of Earth's sphere of influence (SOI) gave the patch conditions of the Mars-Earth trajectory. The arrival conditions for the interplanetary trajectory had to be expressed in such a way that they could be input into POST to run aerocapture simulations starting at the edge of the SOI. The initial position data could be entered in terms of longitude, declination and radius. This longitude is defined with respect to the Greenwich meridian and is equal to the right ascension of the vehicle at 00:00 GMT; its value could be calculated directly

from data supplied by the interplanetary routine. (Actually, any initial longitude would work, since the right ascension does not change appreciably for some time after the vehicle passes into Earth's SOI.) Also, the declination was given in reference to Earth's equatorial plane. With the declination, the longitude, and the radius of the sphere of influence, the position of the vehicle in three-dimensional space was defined. The next step was to determine the value of the entry angle both at the edge of the SOI and at the atmospheric interface for a mid-corridor trajectory. (Remember that the atmospheric interface was considered to be at an altitude of 121.9 km.) For the given V_∞, the entry velocity was calculated and simulations were run with POST to determine the corridor bounds at the atmospheric interface (AI). For further simulations, only the mid-corridor entry angle was considered. However, the entry angle at the atmospheric interface is not equal to that at the edge of the sphere of influence. By looking at the approach geometry, the following equation can be determined for the entry angle as measured at the edge of the SOI:

$$\gamma_{SOI} = 90° - \arcsin\left(\frac{b}{r_{SOI}}\right) \qquad eq.(1)$$

where: b = offset distance[km]

The offset distance is defined as the distance from a line tangent to the approach vector to a parallel line that passes through the center of the Earth (see Figure 21).

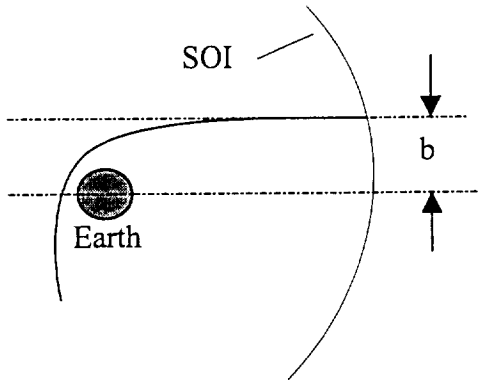

Figure 21. Offset distance of the arrival vector

The value of the offset distance which corresponds to a given atmospheric entry angle can be determined using the angular momentum as given below:

$$H_{SOI} = H_{ai} = \quad v_\infty \cdot b = r_{ai} \cdot v_{ai} \cdot \cos\gamma_{ai} \qquad eq.(2)$$

For a given value of V_∞, the atmospheric entry speed can be determined, and eq. 2 can be used to calculate the entry angle at the edge of the SOI for a specific atmospheric entry angle (in this case, for the mid-corridor angle). The last variable that must be specified for the POST simulations is the azimuth of the velocity vector. It is assumed that while the spacecraft is far from Earth, it is possible to choose the both the azimuth and the flight path angle using a small propulsive maneuver. A specific value of the flight path angle had to be selected at the edge of the SOI to a produce certain entry angle at the atmospheric interface; however, it was not necessary to specify the initial flight azimuth, and this parameter was left as a control.

To gain a better understanding how the azimuth of the velocity vector at the edge of the SOI, the azimuth during atmospheric entry, the final inclination of the parking orbit and the declination of the vehicle upon entering the SOI are related, several trajectory

simulations were done with POST. These simulations calculated the orbital parameters for a hyperbolic trajectory starting at the edge of the sphere of influence for a case with a perigee altitude of around 440 km. If a tangential retro-propulsive burn were performed at the perigee, the vehicle would capture into an orbit around Earth with a certain inclination. Data obtained from these simulations is presented in Figure 22 in which the orbital inclination is shown as a function of the chosen azimuth at the edge of the sphere of influence for various arrival declinations. Note that the declination will vary between approximately $\pm 23.5°$ when the interplanetary trajectory lies in or close to the ecliptic plane.

Aerocapture Simulations Starting at the SOI

To provide an acceptable computation time for the aerocapture simulations starting at the edge of Earth's sphere of influence, the input deck had to be altered. During the first part of the simulation (corresponding to a vehicle radius ranging from approximately 1,000,000 km to 500,000 km), it was expected that the conditions along the trajectory would not change quickly. Therefore, the integration time step size was set to an initial value of 100 seconds. Coming closer to Earth, the trajectory started to curve more and more, so a 50 seconds time step was used from 500,000 to 100,000 km. At 100,000 km the time step size was reduced to 1 second. This step size was used for the rest of the simulation. The adequacy of this variable time step system was verified by running a trajectory with a constant Δt of 1 second. The results for this case compared closely with those using a variable Δt scheme. Except for this change, the input deck was

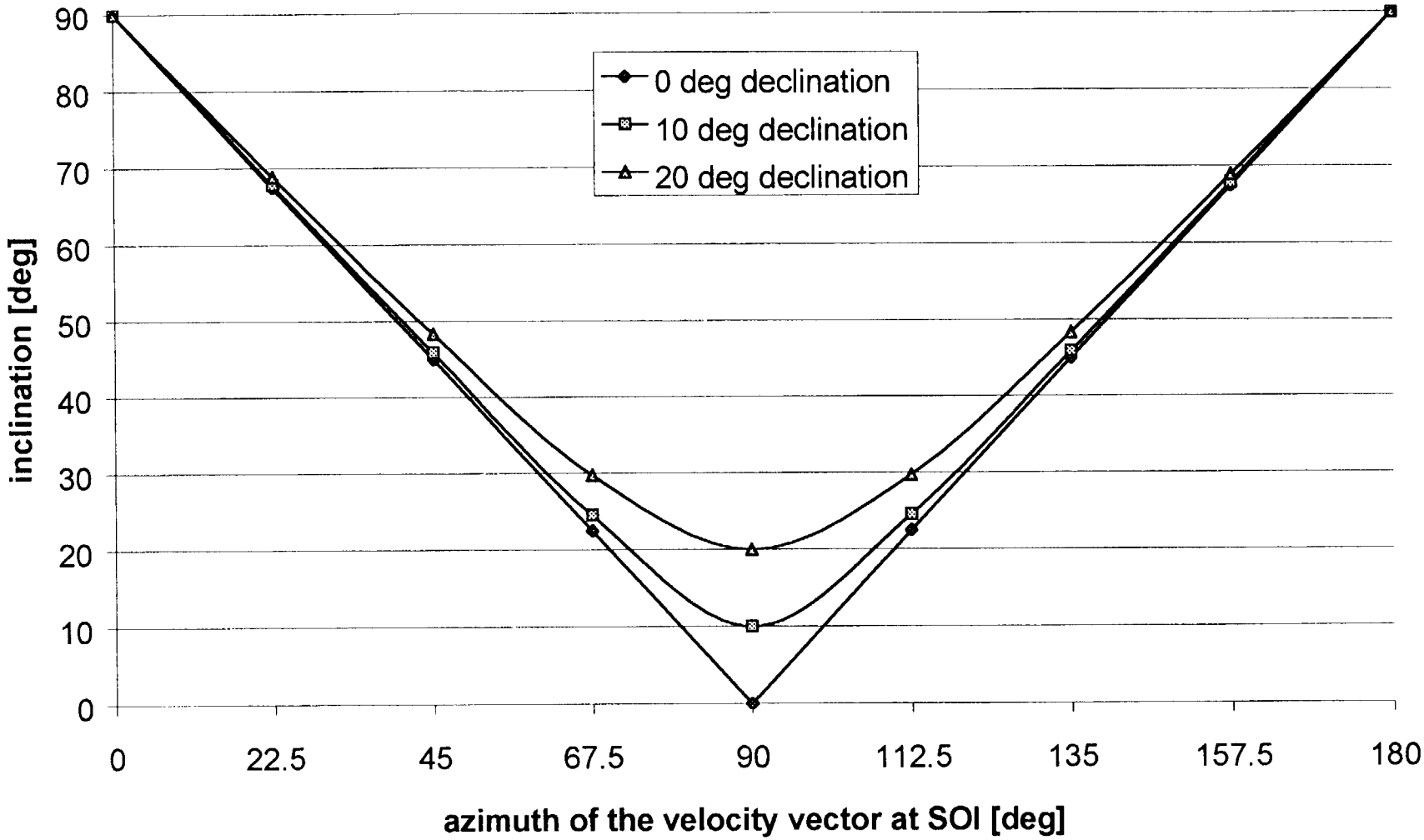

Figure 22. Inclinations achievable with no orbital plane change for various arrival declinations

essentially the same as those used for previous simulations which targeted inclined parking orbits and used the transitional flow and free molecular flow aerodynamics.

With the previously mentioned equations and the data provided by NASA MSFC, the following values were calculated for the entry state at the edge of the sphere of influence: r_{SOI} = 924,657.432 km, longitude = 82.3° and declination = -0.7°. The approach velocity was equal to V_∞ = 4.3845 km/s, and the initial flight path angle at the edge of the SOI was γ_{SOI} = -88.914°. The controls POST used target parking orbits with various inclinations were the azimuth of the velocity vector at the edge of the sphere of influence and the bank angle modulation scheme. The results for these simulations are presented in Table 7. It is apparent that using the three roll sequence, it was possible to target parking orbits with a wide range of inclination. However, it must be remembered that the inclination of the parking orbit cannot be smaller then the arrival declination without requiring an orbital plane change. For the case shown in Table 7, the arrival declination was -0.7°, and therefore, it was possible to capture into essentially any inclination orbit. Preliminary studies have shown that inclinations might be changed using the vehicle's aerodynamic capability by 2 to 3 degrees. Therefore, if the arrival declination has a value of 8° or more, it is unlikely that the T/E with its current configuration and bank angle modulation scheme would be able to capture into the 5.3° inclination orbit above Korou. This work should be carried out for other interplanetary approach vectors with higher values of the declination and arrival velocity.

target inc [deg]	v_{al} [km/sec]	v_{SOI} [km/sec]	γ_{SOI} [deg]	γ_{AI} [deg]	AoA [deg]	azimuth [deg] (90=East)
51.6	11.915	4.385	-88.914	-5.709	45.000	143.605
28.5	11.915	4.385	-88.914	-5.709	45.000	122.438
5.3	11.915	4.385	-88.914	-5.709	45.000	98.267

target inc [deg]	$T1_{roll\_start}$ [sec]	TR1 (turn rate) [deg/sec]	$T1ST_{roll\_stop}$ [sec]	$T2_{roll\_start}$ [sec]	TR2 (turn rate) [deg/sec]	$T2ST_{roll\_stop}$ [sec]
51.6	33.467	-4.506	36.402	15.293	-2.423	24.645
28.5	49.435	-4.960	43.771	15.036	-2.493	24.971
5.3	56.696	-6.000	44.521	15.014	-2.497	24.988

target inc [deg]	$T3_{roll\_start}$ [sec]	TR3 (turn rate) [deg/sec]	$T3ST_{roll\_stop}$ [sec]
51.6	30.057	-5.000	60.900
28.5	29.990	-5.002	60.998
5.3	30.000	-4.992	60.999

target inc [deg]	peak decele-ration[g]	time [sec]	inc [deg]	period [min]	apogee alt [km]	perigee alt [km]
51.6	4.423	201459.098	51.602	88.602	407.406	24.601
28.5	4.349	201224.739	28.491	88.004	413.316	-40.637
5.3	3.868	201178.558	5.304	88.231	419.353	-24.089

Table 7. Bank angle modulation scheme and orbital parameters for aerocapture simulations starting at the edge of the sphere of influence

The possibility of targeting the longitude of the ascending node (LAN) of the parking orbit was briefly examined. After a targeted solution was found for the energy and inclination, an optimization was run by POST to maximize and minimize the LAN. The results showed that the LAN varied only by approximately $\pm 1°$ for the maximum and minimum value that could be obtained. In an attempt to achieve a wider range of the final LAN, the azimuth at the edge of the SOI and the bank angle modulation scheme were varied by large amounts, but this produced no significant improvement. It is likely that an additional control such as a pitch modulation would have to be implemented into the trajectory to satisfy the additional constraint on the longitude of the ascending node. A potentially applicable scheme using a blended roll/pitch control strategy has recently been developed by Jits and Walberg of North Carolina State University (Ref. 5).

Conclusions and Recommendations

This paper reports the results of a preliminary aerocapture study for the TransHab/Ellipsled vehicle upon Earth return from a manned Mars mission. Undershoot and overshoot boundaries have been determined for a range of entry velocities, and the effects of variations in the atmospheric density profile, the vehicle deceleration limit, the maximum vehicle roll rate, the target orbit, and the vehicle ballistic coefficient have been examined. It was found that if a 5-G deceleration limit is used, the TransHab/Ellipsled has a nominal corridor width of at least 0.7 degrees for entry speeds up to 14.0 km/s. This exceeds the corridor width for an Apollo-style capsule slightly. The effects of free-molecular and transitional aerodynamics were evaluated for the TransHab vehicle and were found to be minimal. Entry corridor width was determined as a function of the ballistic coefficient and showed no significant variation at a given entry speed.

A three-roll sequence was implemented to target not only a specific orbital energy, but also a particular inclination, thereby decreasing propulsive inclination changes and the post-aerocapture delta-V. This roll sequence was able to capture the vehicle into a circular parking orbit with an inclination ranging from 5.3 to 51.6 degrees. This same roll control sequence was employed in simulations starting at the edge of Earth's SOI, using the interplanetary approach vector for a 2020 fast-transit return. This assured that realistic entry latitude/azimuth combinations were used when specific inclination orbits were targeted. In these cases, POST was able to target the desired orbital inclinations successfully, using the three-roll sequence and an appropriate choice of the vehicle azimuth at the edge of the SOI.

It was shown that capture into a highly elliptical parking orbit may also be possible; such a strategy would reduce the integrated heat load during aerocapture slightly and would result in a lower ΔV for the trans-Mars injection at the next mission opportunity. However, precise alignment of the target orbit with respect to the subsequent departure hyperbola would be required.

A brief attempt was made to target not only the orbital energy and inclination, but also the longitude of the ascending node (LAN). The bank angle modulation scheme developed for this study was able to influence the LAN only slightly, and it is probable that another control scheme, possibly including angle-of-attack modulation, will be required before significant improvement is seen.

Further aerocapture studies of the TransHab/Ellipsled configuration should address several topics. In order to size the thermal protection system, the maximum heat rates and integrated heat loads should be determined for off stagnation-point areas. Additionally, stagnation-point peak heating rate and integrated heat load could be used as optimization parameters for POST simulations. A reduction of the aerodynamic heating would reduce the TPS size and the total weight of the vehicle. It is conceivable that with the use of a multi-pass aerocapture and new, high-temperature materials, a reusable TPS could be employed on the TransHab/Ellipsled; this possibility should be explored.

To improve orbital targeting abilities, a blended roll/pitch control scheme similar to that developed by Jits and Walberg for Mars aerocapture should be evaluated for Earth return. Using this approach, it may be possible to achieve a wider range of longitude of the ascending node, while still capturing into an orbit with a specific energy and inclination. A second benefit of an AoA modulation scheme could be a further reduction

of the post-aerocapture ΔV. In order to determine the propellant mass required for the TransHab/Ellipsled more accurately, fuel consumption for the aerocapture control system maneuvers should be examined. The effects of atmospheric and aerodynamic dispersions will require more in-depth evaluation using inner/outer loop POST simulations.

The feasibility of capture into a highly elliptical orbit should be studied further, with particular attention to: 1) the added mission complexity which would result from the need to align the aerocapture target orbit with respect to the departure vector for the subsequent mission opportunity, and 2) potential reductions in propellant requirements for the next trans-Mars injection.

References

1) Brauer, G. L., Cornick, D. E., Olson, D. W., Petersen, F. M. and Stevenson, R.; "Program to Optimize Simulated Trajectories (POST), Volume I, Formulation Manual" Martin Marietta Corporation, September 1990.

2) Sutton, K. and Hartung, L. C.; "Equilibrium Radiative Heating Tables for Earth Entry"; NASA Technical Memorandum 102 652, NASA Langley Research Center, Hampton, VA, May 1990.

3) Wilmoth, R. G., Mitcheltree, R. A. and Moss, J. N.; "Low-Density Aerodynamics of the Stardust Sample Return Capsule"; Journal of Spacecraft and Rockets, Vol. 36, No. 3, May-June 1999, pp. 436-441.

4) Drake, Bret G., and Cooke, Douglas R. (Editors); "Reference Mission Version 3.0, Addendum to the Human Exploration of Mars: The Reference Mission of the NASA Mars Exploration Study Team"; Houston, Texas, 1998.
http://spaceflight.nasa.gov/mars/reference/hem/hem2.html

5) Jits, R. and G. Walberg, "A Blended Two-Axis Control Scheme for Use in the Aerocapture of Vehicles at Mars," Graduate Seminar, University of Tennessee, Knoxville, TN, December 2, 1999.